Halo formation of the gaussian density beam in periodic solenoidal focusing field

61th ICFA Advanced Beam Dynamics Workshop
on High-intensity and High-brightness Hadron beams (**HB 2018**)
In Daejeon

Yoolim Cheon and Moses Chung,
Intense Beam and Accelerator Laboratory (IBAL),
Ulsan National Institute of Science and Technology (UNIST)

Contents

High-intensity charged-particle beam physics

Applications

High-intensity charged-particle beam physics

Applications

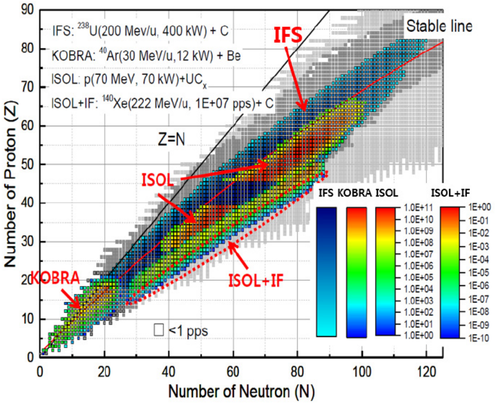

High-intensity charged-particle beam physics

Applications

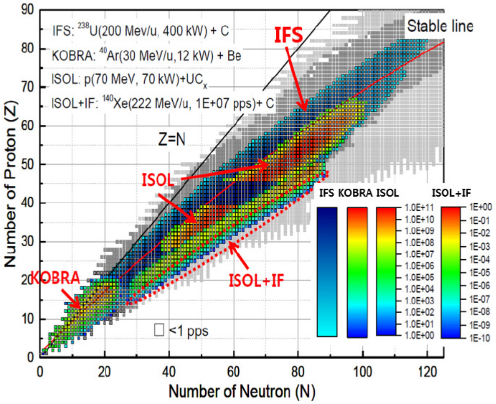

astrophysical nuclear reactions carrying the nucleosynthetic processes and nuclear properties

High-intensity charged-particle beam physics

Applications

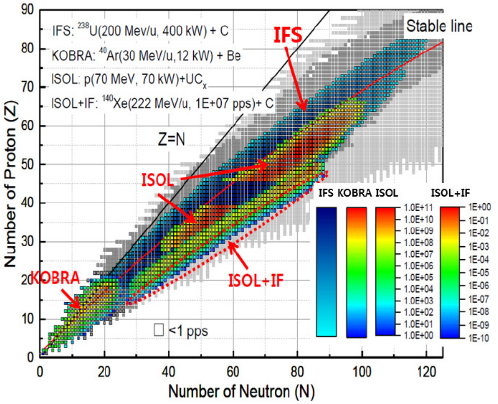

astrophysical nuclear reactions
carrying the nucleosynthetic
processes and nuclear properties

High-intensity charged-particle beam physics

Applications

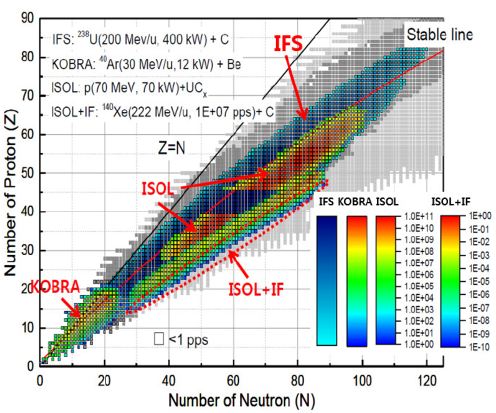

astrophysical nuclear reactions carrying the nucleosynthetic processes and nuclear properties

high energy particle physics

High-intensity charged-particle beam physics

Applications

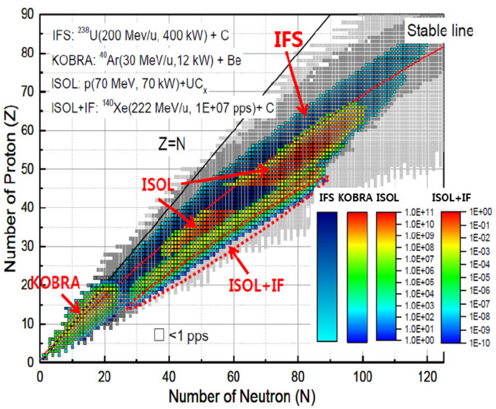

astrophysical nuclear reactions carrying the nucleosynthetic processes and nuclear properties

high energy particle physics

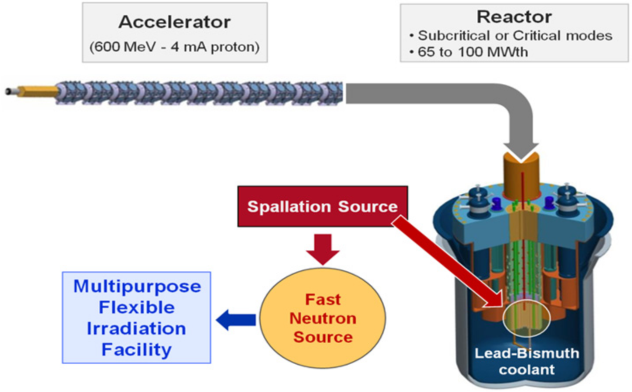

High-intensity charged-particle beam physics

Applications

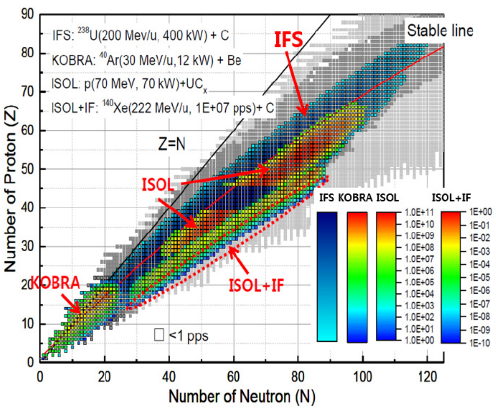

astrophysical nuclear reactions carrying the nucleosynthetic processes and nuclear properties

high energy particle physics

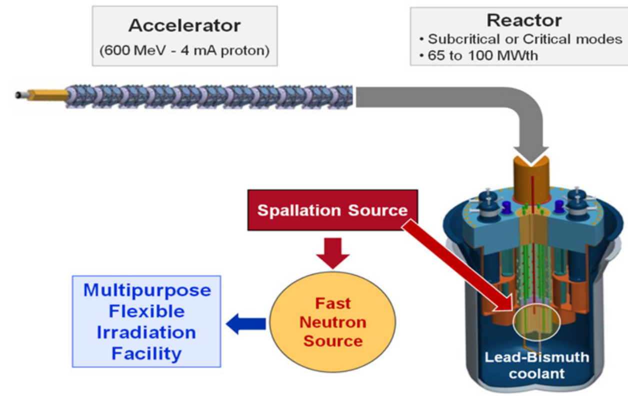

nuclear waste transmutation

High-intensity charged-particle beam physics

Applications

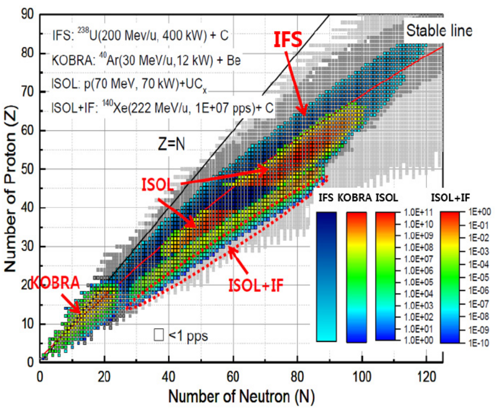

astrophysical nuclear reactions carrying the nucleosynthetic processes and nuclear properties

high energy particle physics

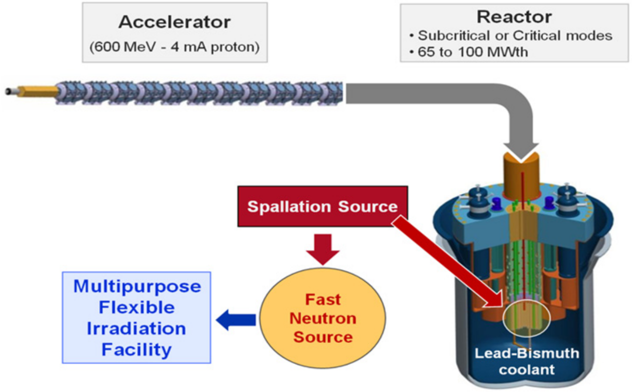

nuclear waste transmutation

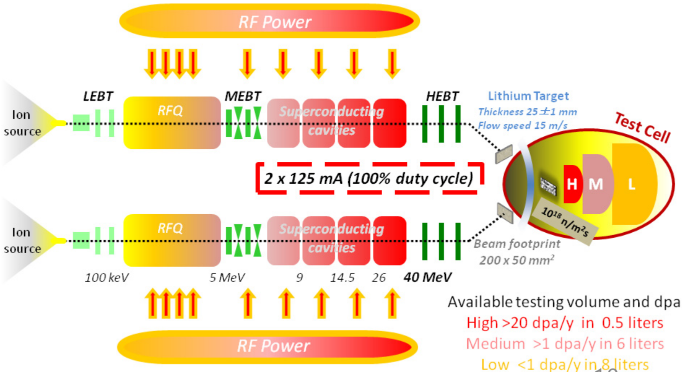

High-intensity charged-particle beam physics

Applications

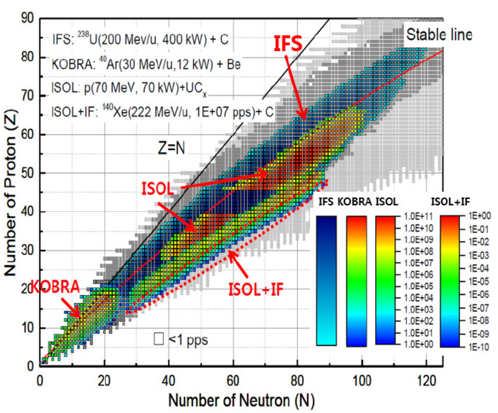

astrophysical nuclear reactions carrying the nucleosynthetic processes and nuclear properties

high energy particle physics

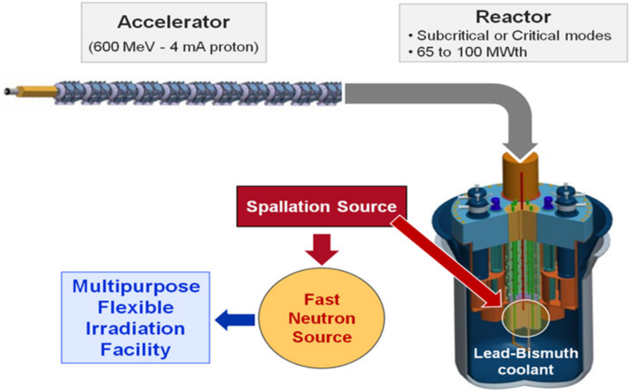

nuclear waste transmutation

fusion material test (IFMIF)

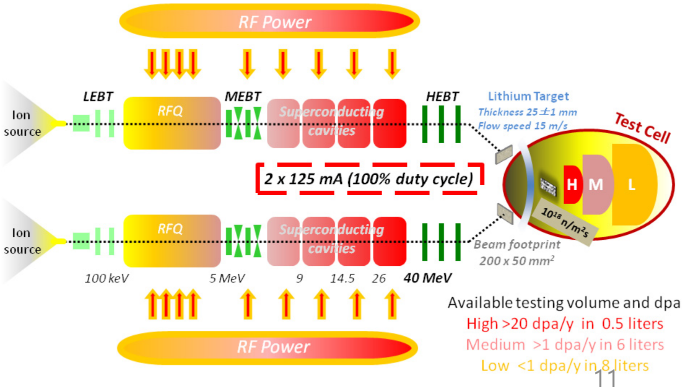

High-intensity charged-particle beam physics

Applications

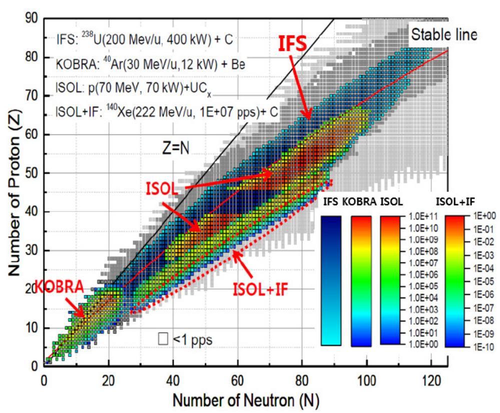

astrophysical nuclear reactions carrying the nucleosynthetic processes and nuclear properties

high energy particle physics

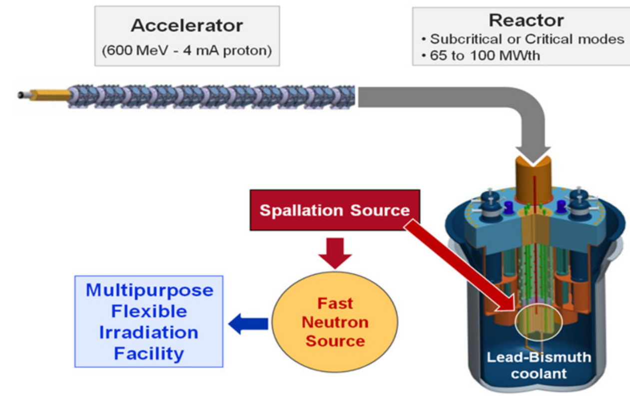

nuclear waste transmutation

fusion material test
(IFMIF)

HWR - Solenoidal focusing

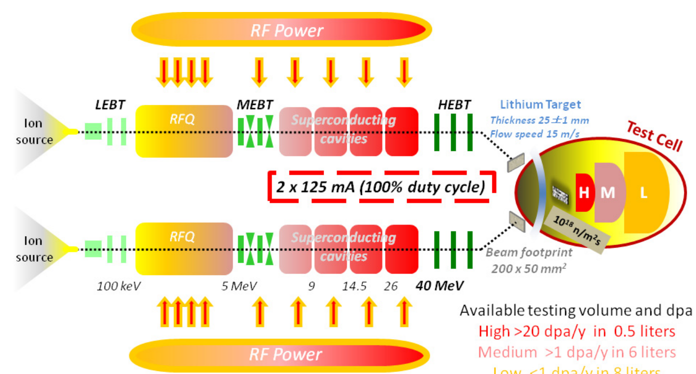

High-intensity charged-particle beam physics

Periodic solenoidal focusing field

High-intensity charged-particle beam physics

Periodic solenoidal focusing field

- **Periodic solenoidal focusing field**

Periodic solenoidal focusing field

- **Periodic solenoidal focusing field**

$$\boldsymbol{\kappa_z(s) = \kappa_z(s+S) = \left(\frac{B_{Z0}(s)}{2[B\rho]}\right)^2 = \left(\frac{\omega_c(s)}{2\gamma_b\beta_b c}\right)^2}$$

Periodic solenoidal focusing field

- **Periodic solenoidal focusing field**

$$\boldsymbol{\kappa_z(s) = \kappa_z(s+S) = \left(\frac{B_{Z0}(s)}{2[B\rho]}\right)^2 = \left(\frac{\omega_c(s)}{2\gamma_b\beta_b c}\right)^2}$$

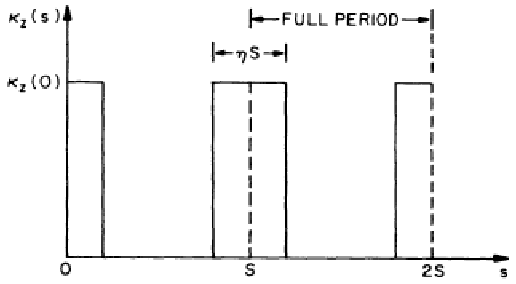

High-intensity charged-particle beam physics

Periodic solenoidal focusing field

- **Periodic solenoidal focusing field**

$$\kappa_z(s) = \kappa_z(s+S) = \left(\frac{B_{Z0}(s)}{2[B\rho]}\right)^2 = \left(\frac{\omega_c(s)}{2\gamma_b\beta_b c}\right)^2$$

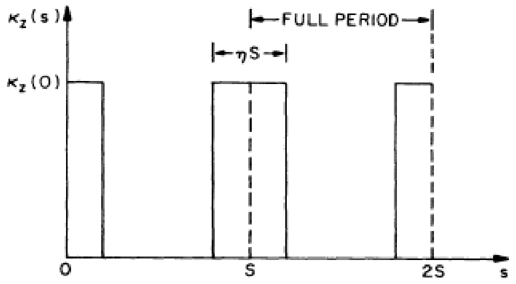

- The dynamics of the charged particle is easily analyzed in the **Larmour frame**, which rotates with the Larmour frequency around the axis of the solenoid
- Much simpler and cheaper
- **Rotationally symmetric**
- For a given beam emittance, the solenoid aperture required is smaller than that of the quadrupole

High-intensity charged-particle beam physics

Periodic solenoidal focusing field

- **Periodic solenoidal focusing field**

$$\boldsymbol{\kappa_z(s) = \kappa_z(s+S) = \left(\frac{B_{Z0}(s)}{2[B\rho]}\right)^2 = \left(\frac{\omega_c(s)}{2\gamma_b\beta_b c}\right)^2}$$

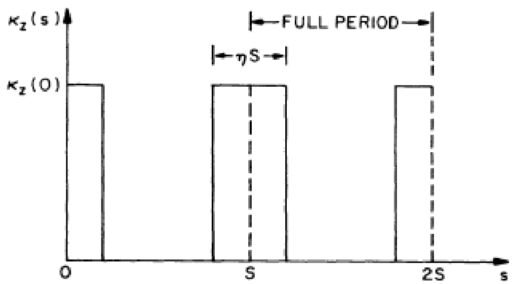

- The dynamics of the charged particle is easily analyzed in the **Larmour frame**, which rotates with the Larmour frequency around the axis of the solenoid
- Much simpler and cheaper
- **Rotationally symmetric**
- For a given beam emittance, the solenoid aperture required is smaller than that of the quadrupole

- **Normalized envelope equation**

➢ Introduce the dimensionless parameters and variables,

$$\frac{s}{S} \to s, \qquad \frac{r_b}{\sqrt{\epsilon S}} \to r_b, \qquad S^2\kappa_z \to \kappa_z, \qquad \frac{SK}{\epsilon} \to K$$

➢ With **symmetric** envelope radius, $r_x(s) = r_y(s) \equiv r_b(s)$

➢ **The normalized envelope equation**

$$r_b''(s) + \kappa_z(s) r_b(s) - \frac{K}{r_b(s)} - \frac{1}{r_b^3(s)} = 0$$

➢ Space charge defocusing; $K \equiv \frac{2q\lambda}{\gamma_b^3 \beta_b^2 mc^2}$: Perveance

➢ $\sigma_0 \equiv \int_0^1 \sqrt{\kappa_z(s)}\, ds = \int_0^1 \sqrt{\eta\kappa_z(0)}\, ds = \sqrt{\eta\kappa_z(0)}$

: undepressed (vacuum) phase advance

(normalized)

➢ $\sigma \equiv \int_0^1 \frac{ds}{r_b^2(s)}$: depressed phase advance

High-intensity charged-particle beam physics

Nonlinear resonances and chaotic motions of envelope oscillation

Envelope oscillations

(phase plane r_b -$r_b{}'$)

$$r_b{}''(s) + \kappa_z(s) r_b(s) - \frac{K}{r_b(s)} - \frac{1}{r_b{}^3(s)} = 0$$

Space charge perveance (K)	Focusing field parameter	Vacuum phase advance (σ_0)	Matched beam initial condition
0	$\kappa_z(0) = 3.79$,$\eta = \frac{1}{6}$	45.5°	$\boldsymbol{r_b}(0) = 1.16$,$\boldsymbol{r'_b}(0) = 0$
3	$\kappa_z(0) = 3.79$,$\eta = \frac{1}{6}$	45.5°	$\boldsymbol{r_b}(0) = 2.3$,$\boldsymbol{r'_b}(0) = 0$
5	$\kappa_z(0) = 24.2$,$\eta = \frac{1}{6}$	115°	$\boldsymbol{r_b}(0) = 1.4$,$\boldsymbol{r'_b}(0) = 0$

High-intensity charged-particle beam physics

Nonlinear resonances and chaotic motions of envelope oscillation

Envelope oscillations

(phase plane r_b -$r_b{}'$)

$$r_b{}''(s) + \kappa_z(s) r_b(s) - \frac{K}{r_b(s)} - \frac{1}{r_b{}^3(s)} = 0$$

Space charge perveance (K)	Focusing field parameter	Vacuum phase advance (σ_0)	Matched beam initial condition
0	$\kappa_z(0) = 3.79$,$\eta = \frac{1}{6}$	45.5°	$\boldsymbol{r_b}(0) = 1.16$,$\boldsymbol{r'_b}(0) = 0$
3	$\kappa_z(0) = 3.79$,$\eta = \frac{1}{6}$	45.5°	$\boldsymbol{r_b}(0) = 2.3$,$\boldsymbol{r'_b}(0) = 0$
5	$\kappa_z(0) = 24.2$,$\eta = \frac{1}{6}$	115°	$\boldsymbol{r_b}(0) = 1.4$,$\boldsymbol{r'_b}(0) = 0$

High-intensity charged-particle beam physics

Nonlinear resonances and chaotic motions of envelope oscillation

Envelope oscillations

(phase plane r_b -r_b')

$$r_b''(s) + \kappa_z(s) r_b(s) - \frac{K}{r_b(s)} - \frac{1}{r_b{}^3(s)} = 0$$

Space charge perveance (K)	Focusing field parameter	Vacuum phase advance (σ_0)	Matched beam initial condition
0	$\kappa_z(0) = 3.79$,$\eta = \frac{1}{6}$	45.5°	$\boldsymbol{r_b}(0) = 1.16$,$\boldsymbol{r_b'}(0) = 0$
3	$\kappa_z(0) = 3.79$,$\eta = \frac{1}{6}$	45.5°	$\boldsymbol{r_b}(0) = 2.3$,$\boldsymbol{r_b'}(0) = 0$
5	$\kappa_z(0) = 24.2$,$\eta = \frac{1}{6}$	115°	$\boldsymbol{r_b}(0) = 1.4$,$\boldsymbol{r_b'}(0) = 0$

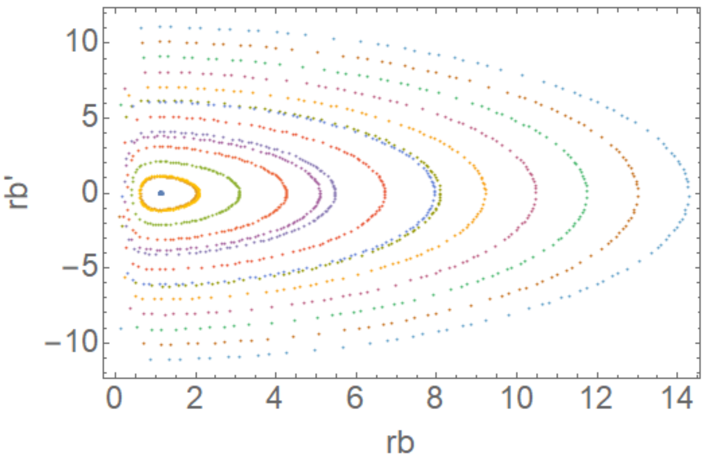

High-intensity charged-particle beam physics

Nonlinear resonances and chaotic motions of envelope oscillation

All points are plotted **in every S lattice period** (Poincare surface of section plots) with different envelope initial conditions for propagation **over 300 lattice periods**

Envelope oscillations

(phase plane r_b -$r_b{}'$)

$$r_b{}''(s) + \kappa_z(s) r_b(s) - \frac{K}{r_b(s)} - \frac{1}{r_b{}^3(s)} = 0$$

Space charge perveance (K)	Focusing field parameter	Vacuum phase advance (σ_0)	Matched beam initial condition
0	$\kappa_z(0) = 3.79$,$\eta = \frac{1}{6}$	45.5°	$\boldsymbol{r_b}(0) = 1.16$,$\boldsymbol{r'_b}(0) = 0$
3	$\kappa_z(0) = 3.79$,$\eta = \frac{1}{6}$	45.5°	$\boldsymbol{r_b}(0) = 2.3$,$\boldsymbol{r'_b}(0) = 0$
5	$\kappa_z(0) = 24.2$,$\eta = \frac{1}{6}$	115°	$\boldsymbol{r_b}(0) = 1.4$,$\boldsymbol{r'_b}(0) = 0$

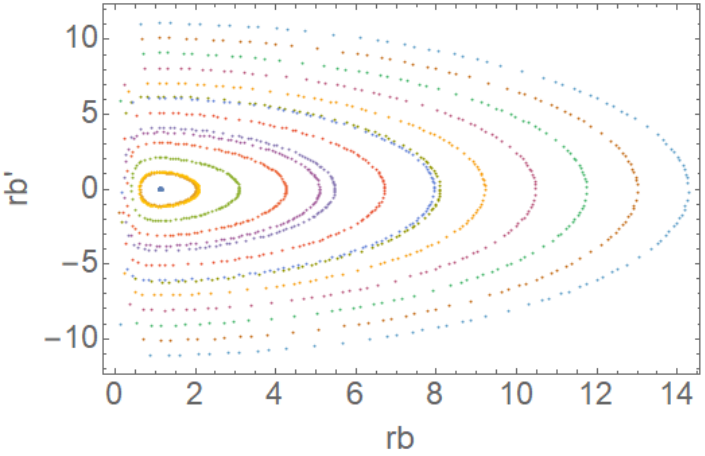

High-intensity charged-particle beam physics

Nonlinear resonances and chaotic motions of envelope oscillation

All points are plotted **in every S lattice period** (Poincare surface of section plots) with different envelope initial conditions for propagation **over 300 lattice periods**

Envelope oscillations

(phase plane r_b -r_b')

$$r_b''(s) + \kappa_z(s) r_b(s) - \frac{K}{r_b(s)} - \frac{1}{r_b^{\,3}(s)} = 0$$

Space charge perveance (K)	Focusing field parameter	Vacuum phase advance (σ_0)	Matched beam initial condition
0	$\kappa_z(0) = 3.79, \eta = \frac{1}{6}$	45.5°	$r_b(0) = 1.16, r_b'(0) = 0$
3	$\kappa_z(0) = 3.79, \eta = \frac{1}{6}$	45.5°	$r_b(0) = 2.3, r_b'(0) = 0$
5	$\kappa_z(0) = 24.2, \eta = \frac{1}{6}$	115°	$r_b(0) = 1.4, r_b'(0) = 0$

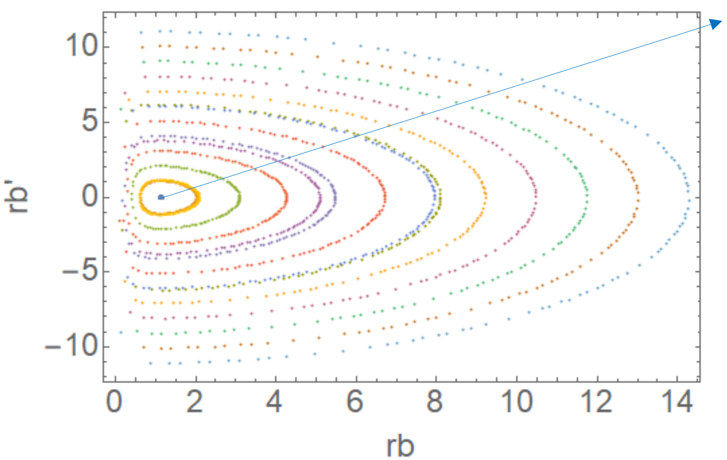

High-intensity charged-particle beam physics

Nonlinear resonances and chaotic motions of envelope oscillation

All points are plotted **in every S lattice period** (Poincare surface of section plots) with different envelope initial conditions for propagation **over 300 lattice periods**

Envelope oscillations

(phase plane r_b -r_b')

$$r_b''(s) + \kappa_z(s) r_b(s) - \frac{K}{r_b(s)} - \frac{1}{{r_b}^3(s)} = 0$$

Space charge perveance (K)	Focusing field parameter	Vacuum phase advance (σ_0)	Matched beam initial condition
0	$\kappa_z(0) = 3.79, \eta = \frac{1}{6}$	45.5°	$r_b(0) = 1.16, r_b'(0) = 0$
3	$\kappa_z(0) = 3.79, \eta = \frac{1}{6}$	45.5°	$r_b(0) = 2.3, r_b'(0) = 0$
5	$\kappa_z(0) = 24.2, \eta = \frac{1}{6}$	115°	$r_b(0) = 1.4, r_b'(0) = 0$

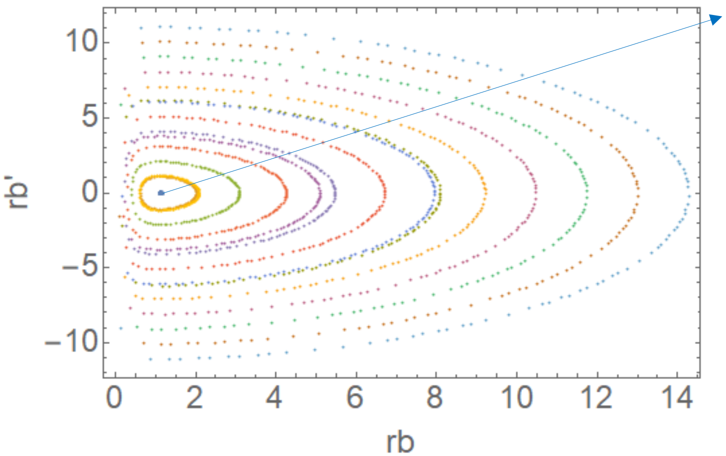

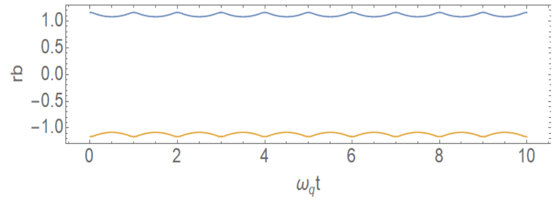

High-intensity charged-particle beam physics

Nonlinear resonances and chaotic motions of envelope oscillation

All points are plotted **in every S lattice period** (Poincare surface of section plots) with different envelope initial conditions for propagation **over 300 lattice periods**

Envelope oscillations

(phase plane r_b -r_b')

$$r_b''(s) + \kappa_z(s) r_b(s) - \frac{K}{r_b(s)} - \frac{1}{{r_b}^3(s)} = 0$$

Space charge perveance (K)	Focusing field parameter	Vacuum phase advance (σ_0)	Matched beam initial condition
0	$\kappa_z(0) = 3.79, \eta = \frac{1}{6}$	45.5°	$r_b(0) = 1.16, r_b'(0) = 0$
3	$\kappa_z(0) = 3.79, \eta = \frac{1}{6}$	45.5°	$r_b(0) = 2.3, r_b'(0) = 0$
5	$\kappa_z(0) = 24.2, \eta = \frac{1}{6}$	115°	$r_b(0) = 1.4, r_b'(0) = 0$

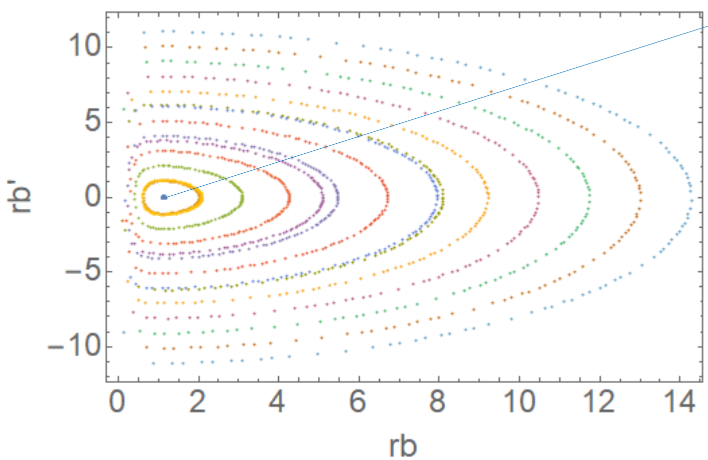

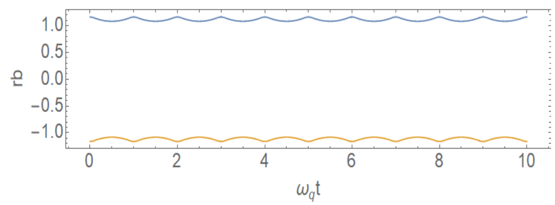

Matched beam in solenoidal focusing

(equilibrium envelope radius)

$$r_b(s) = r_b(s+S) = const.$$

High-intensity charged-particle beam physics

Nonlinear resonances and chaotic motions of envelope oscillation

All points are plotted **in every S lattice period** (Poincare surface of section plots) with different envelope initial conditions for propagation **over 300 lattice periods**

Envelope oscillations

(phase plane r_b -r_b')

$$r_b''(s) + \kappa_z(s) r_b(s) - \frac{K}{r_b(s)} - \frac{1}{r_b^3(s)} = 0$$

Space charge perveance (K)	Focusing field parameter	Vacuum phase advance (σ_0)	Matched beam initial condition
0	$\kappa_z(0) = 3.79, \eta = \frac{1}{6}$	45.5°	$r_b(0) = 1.16, r_b'(0) = 0$
3	$\kappa_z(0) = 3.79, \eta = \frac{1}{6}$	45.5°	$r_b(0) = 2.3, r_b'(0) = 0$
5	$\kappa_z(0) = 24.2, \eta = \frac{1}{6}$	115°	$r_b(0) = 1.4, r_b'(0) = 0$

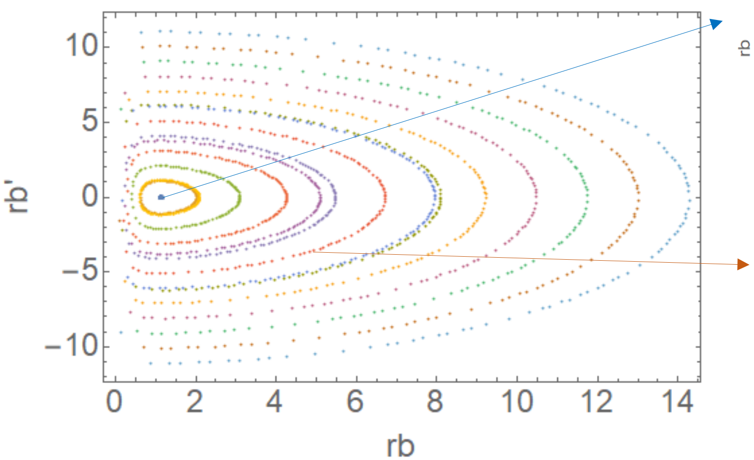

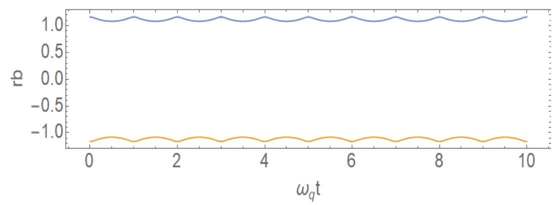

Matched beam in solenoidal focusing

(equilibrium envelope radius)

$$r_b(s) = r_b(s+S) = const.$$

High-intensity charged-particle beam physics

Nonlinear resonances and chaotic motions of envelope oscillation

All points are plotted **in every S lattice period** (Poincare surface of section plots) with different envelope initial conditions for propagation **over 300 lattice periods**

Envelope oscillations

(phase plane r_b -$r_b{}'$)

$$r_b{}''(s) + \kappa_z(s) r_b(s) - \frac{K}{r_b(s)} - \frac{1}{r_b{}^3(s)} = 0$$

Space charge perveance (K)	Focusing field parameter	Vacuum phase advance (σ_0)	Matched beam initial condition
0	$\kappa_z(0) = 3.79$,$\eta = \frac{1}{6}$	45.5°	$\boldsymbol{r_b}(0) = 1.16$,$\boldsymbol{r'_b}(0) = 0$
3	$\kappa_z(0) = 3.79$,$\eta = \frac{1}{6}$	45.5°	$\boldsymbol{r_b}(0) = 2.3$,$\boldsymbol{r'_b}(0) = 0$
5	$\kappa_z(0) = 24.2$,$\eta = \frac{1}{6}$	115°	$\boldsymbol{r_b}(0) = 1.4$,$\boldsymbol{r'_b}(0) = 0$

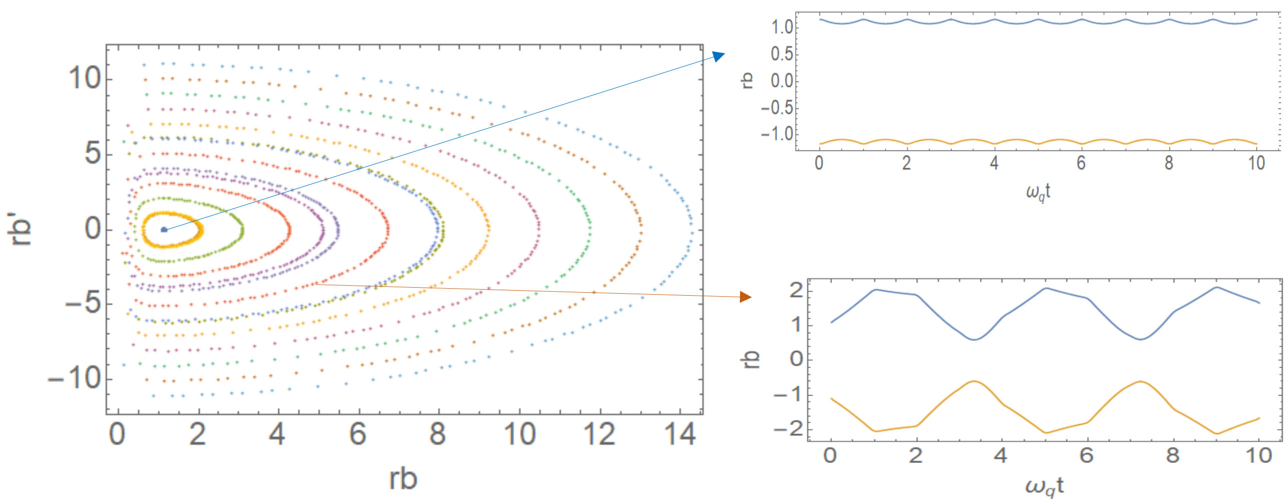

Matched beam in solenoidal focusing

(equilibrium envelope radius)

$$\boldsymbol{r_b(s) = r_b(s+S) = const.}$$

High-intensity charged-particle beam physics

Nonlinear resonances and chaotic motions of envelope oscillation

All points are plotted **in every S lattice period** (Poincare surface of section plots) with different envelope initial conditions for propagation **over 300 lattice periods**

Envelope oscillations

(phase plane r_b -r_b')

$$r_b''(s) + \kappa_z(s) r_b(s) - \frac{K}{r_b(s)} - \frac{1}{{r_b}^3(s)} = 0$$

Space charge perveance (**K**)	Focusing field parameter	Vacuum phase advance (**σ_0**)	**Matched beam** initial condition
0	$\kappa_z(0) = 3.79$,$\eta = \frac{1}{6}$	45.5°	$\boldsymbol{r_b}(0) = 1.16$,$\boldsymbol{r_b'}(0) = 0$
3	$\kappa_z(0) = 3.79$,$\eta = \frac{1}{6}$	45.5°	$\boldsymbol{r_b}(0) = 2.3$,$\boldsymbol{r_b'}(0) = 0$
5	$\kappa_z(0) = 24.2$,$\eta = \frac{1}{6}$	115°	$\boldsymbol{r_b}(0) = 1.4$,$\boldsymbol{r_b'}(0) = 0$

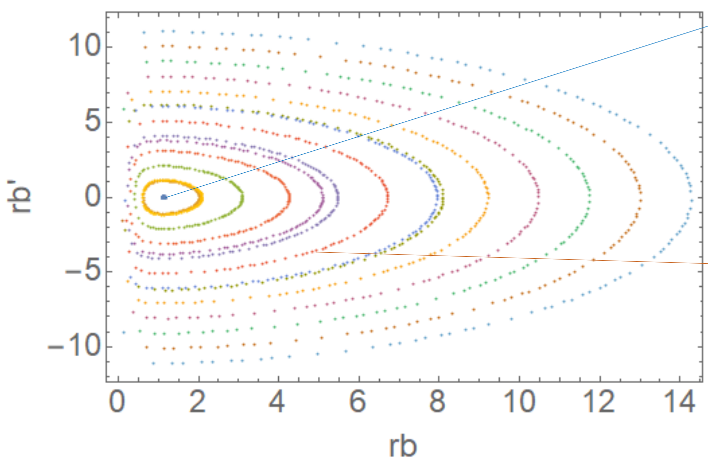

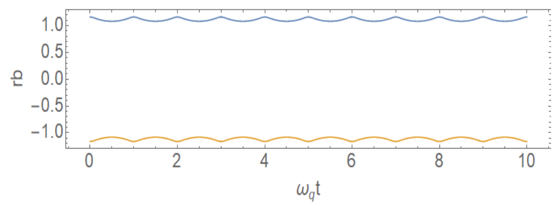

Matched beam in solenoidal focusing

(equilibrium envelope radius)

$$\boldsymbol{r_b(s) = r_b(s+S) = const.}$$

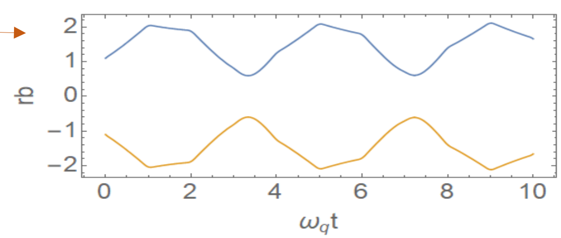

Mismatched beam in solenoidal focusing

$$\boldsymbol{r(s)} = \boldsymbol{r_b}(s; matched) + \boldsymbol{\delta r}$$

High-intensity charged-particle beam physics

Nonlinear resonances and chaotic motions of envelope oscillation

All points are plotted **in every S lattice period** (Poincare surface of section plots) with different envelope initial conditions for propagation **over 300 lattice periods**

Envelope oscillations

(phase plane r_b -$r_b{}'$)

$$r_b{}''(s) + \kappa_z(s) r_b(s) - \frac{K}{r_b(s)} - \frac{1}{r_b{}^3(s)} = 0$$

Space charge perveance (K)	Focusing field parameter	Vacuum phase advance (σ_0)	Matched beam initial condition
0	$\kappa_z(0) = 3.79$,$\eta = \frac{1}{6}$	45.5°	$r_b(0) = 1.16$,$r_b'(0) = 0$
3	$\kappa_z(0) = 3.79$,$\eta = \frac{1}{6}$	45.5°	$r_b(0) = 2.3$,$r_b'(0) = 0$
5	$\kappa_z(0) = 24.2$,$\eta = \frac{1}{6}$	115°	$r_b(0) = 1.4$,$r_b'(0) = 0$

High-intensity charged-particle beam physics

Nonlinear resonances and chaotic motions of envelope oscillation

All points are plotted **in every S lattice period** (Poincare surface of section plots) with different envelope initial conditions for propagation **over 300 lattice periods**

Envelope oscillations

(phase plane r_b -r_b')

$$r_b''(s) + \kappa_z(s) r_b(s) - \frac{K}{r_b(s)} - \frac{1}{r_b^3(s)} = 0$$

Space charge perveance (K)	Focusing field parameter	Vacuum phase advance (σ_0)	Matched beam initial condition
0	$\kappa_z(0) = 3.79$,$\eta = \frac{1}{6}$	45.5°	$r_b(0) = 1.16$,$r_b'(0) = 0$
3	$\kappa_z(0) = 3.79$,$\eta = \frac{1}{6}$	45.5°	$r_b(0) = 2.3$,$r_b'(0) = 0$
5	$\kappa_z(0) = 24.2$,$\eta = \frac{1}{6}$	115°	$r_b(0) = 1.4$,$r_b'(0) = 0$

High-intensity charged-particle beam physics

Nonlinear resonances and chaotic motions of envelope oscillation

All points are plotted **in every S lattice period** (Poincare surface of section plots) with different envelope initial conditions for propagation **over 300 lattice periods**

Envelope oscillations

(phase plane r_b -r_b')

$$r_b''(s) + \kappa_z(s) r_b(s) - \frac{K}{r_b(s)} - \frac{1}{r_b^3(s)} = 0$$

Space charge perveance (K)	Focusing field parameter	Vacuum phase advance (σ_0)	Matched beam initial condition
0	$\kappa_z(0) = 3.79$,$\eta = \frac{1}{6}$	45.5°	$\boldsymbol{r_b}(0) = 1.16$,$\boldsymbol{r_b'}(0) = 0$
3	$\kappa_z(0) = 3.79$,$\eta = \frac{1}{6}$	45.5°	$\boldsymbol{r_b}(0) = 2.3$,$\boldsymbol{r_b'}(0) = 0$
5	$\kappa_z(0) = 24.2$,$\eta = \frac{1}{6}$	115°	$\boldsymbol{r_b}(0) = 1.4$,$\boldsymbol{r_b'}(0) = 0$

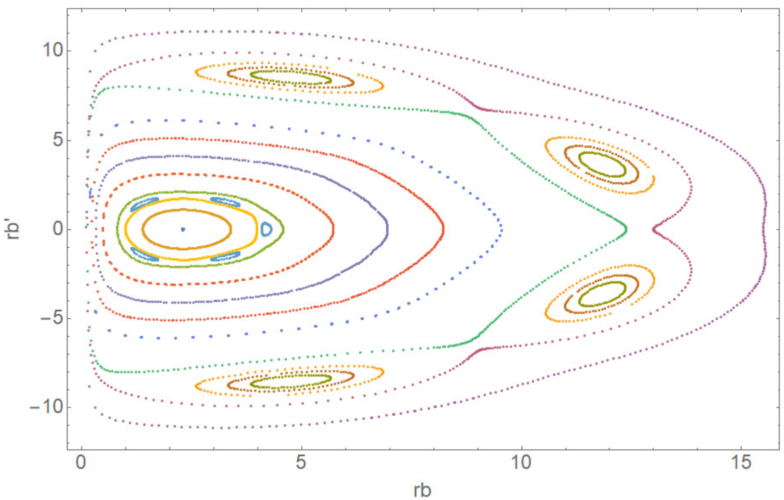

High-intensity charged-particle beam physics

Nonlinear resonances and chaotic motions of envelope oscillation

All points are plotted **in every S lattice period** (Poincare surface of section plots) with different envelope initial conditions for propagation **over 300 lattice periods**

Envelope oscillations

(phase plane r_b -r_b')

$$r_b''(s) + \kappa_z(s) r_b(s) - \frac{K}{r_b(s)} - \frac{1}{r_b{}^3(s)} = 0$$

Space charge perveance (K)	Focusing field parameter	Vacuum phase advance (σ_0)	Matched beam initial condition
0	$\kappa_z(0) = 3.79$,$\eta = \frac{1}{6}$	45.5°	$\boldsymbol{r_b}(0) = 1.16$,$\boldsymbol{r'_b}(0) = 0$
3	$\kappa_z(0) = 3.79$,$\eta = \frac{1}{6}$	45.5°	$\boldsymbol{r_b}(0) = 2.3$,$\boldsymbol{r'_b}(0) = 0$
5	$\kappa_z(0) = 24.2$,$\eta = \frac{1}{6}$	115°	$\boldsymbol{r_b}(0) = 1.4$,$\boldsymbol{r'_b}(0) = 0$

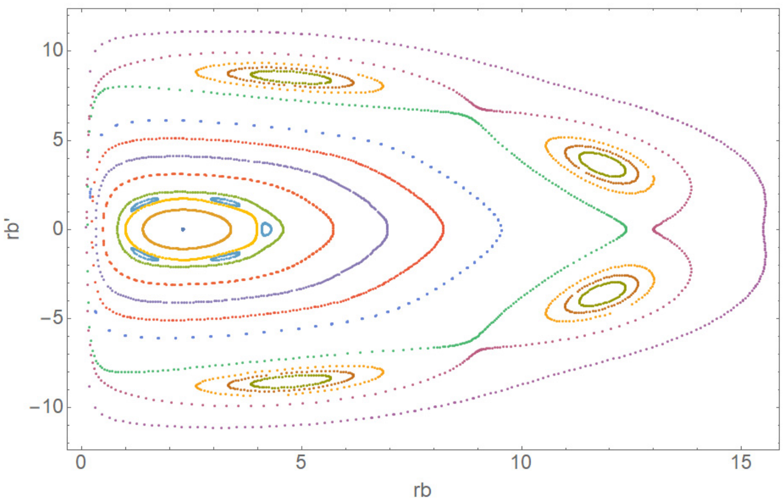

n-th order resonance

$$r(s) = r_b(s; matched) + \delta r \ , \ \delta r(s) = \delta r(0)\boldsymbol{cos}(\boldsymbol{k_n s})$$

High-intensity charged-particle beam physics

Nonlinear resonances and chaotic motions of envelope oscillation

All points are plotted **in every S lattice period** (Poincare surface of section plots) with different envelope initial conditions for propagation **over 300 lattice periods**

Envelope oscillations

(phase plane r_b -$r_b{}'$)

$$r_b{}''(s) + \kappa_z(s) r_b(s) - \frac{K}{r_b(s)} - \frac{1}{r_b{}^3(s)} = 0$$

Space charge perveance (K)	Focusing field parameter	Vacuum phase advance (σ_0)	Matched beam initial condition
0	$\kappa_z(0) = 3.79$,$\eta = \frac{1}{6}$	45.5°	$\boldsymbol{r_b}(0) = 1.16$,$\boldsymbol{r_b'}(0) = 0$
3	$\kappa_z(0) = 3.79$,$\eta = \frac{1}{6}$	45.5°	$\boldsymbol{r_b}(0) = 2.3$,$\boldsymbol{r_b'}(0) = 0$
5	$\kappa_z(0) = 24.2$,$\eta = \frac{1}{6}$	115°	$\boldsymbol{r_b}(0) = 1.4$,$\boldsymbol{r_b'}(0) = 0$

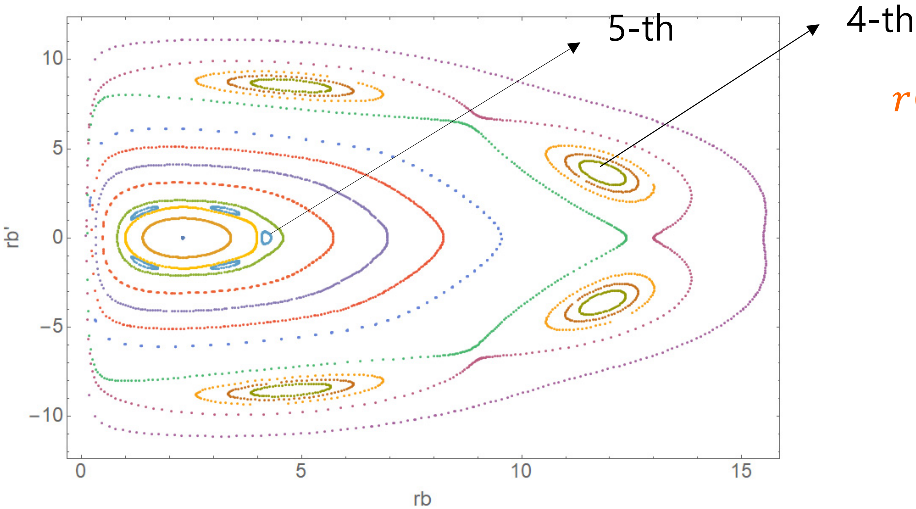

n-th order resonance

$$r(s) = r_b(s; matched) + \delta r \;\;,\;\; \delta r(s) = \delta r(0)\boldsymbol{cos(k_n s)}$$

High-intensity charged-particle beam physics

Nonlinear resonances and chaotic motions of envelope oscillation

All points are plotted **in every S lattice period** (Poincare surface of section plots) with different envelope initial conditions for propagation **over 300 lattice periods**

Envelope oscillations

(phase plane r_b -r_b')

$$r_b''(s) + \kappa_z(s) r_b(s) - \frac{K}{r_b(s)} - \frac{1}{{r_b}^3(s)} = 0$$

Space charge perveance (K)	Focusing field parameter	Vacuum phase advance (σ_0)	Matched beam initial condition
0	$\kappa_z(0) = 3.79$,$\eta = \frac{1}{6}$	45.5°	$\boldsymbol{r_b}(0) = 1.16$,$\boldsymbol{r_b'}(0) = 0$
3	$\kappa_z(0) = 3.79$,$\eta = \frac{1}{6}$	45.5°	$\boldsymbol{r_b}(0) = 2.3$,$\boldsymbol{r_b'}(0) = 0$
5	$\kappa_z(0) = 24.2$,$\eta = \frac{1}{6}$	115°	$\boldsymbol{r_b}(0) = 1.4$,$\boldsymbol{r_b'}(0) = 0$

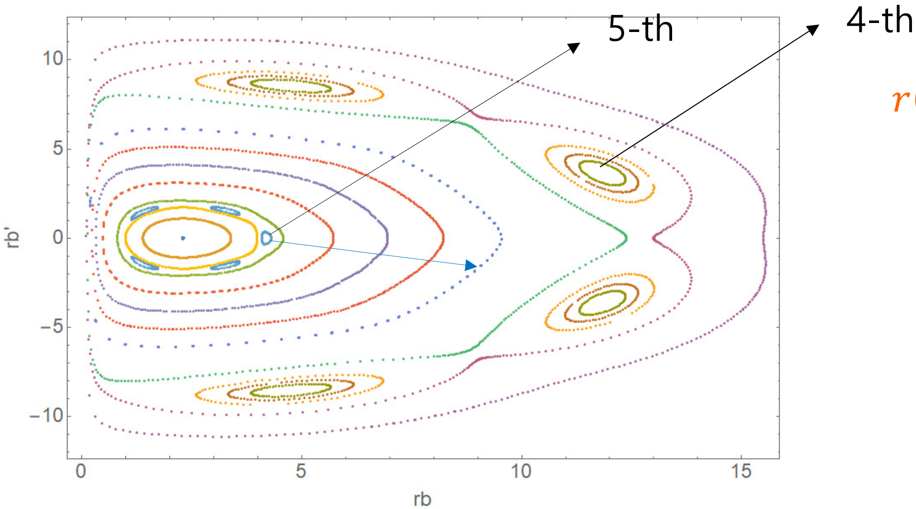

n-th order resonance

$$r(s) = r_b(s; matched) + \delta r \ , \ \delta r(s) = \delta r(0) \boldsymbol{cos}(\boldsymbol{k_n s})$$

High-intensity charged-particle beam physics

Nonlinear resonances and chaotic motions of envelope oscillation

All points are plotted **in every S lattice period** (Poincare surface of section plots) with different envelope initial conditions for propagation **over 300 lattice periods**

Envelope oscillations

(phase plane r_b -r_b')

$$r_b''(s) + \kappa_z(s) r_b(s) - \frac{K}{r_b(s)} - \frac{1}{{r_b}^3(s)} = 0$$

Space charge perveance (K)	Focusing field parameter	Vacuum phase advance (σ_0)	Matched beam initial condition
0	$\kappa_z(0) = 3.79, \eta = \frac{1}{6}$	45.5°	$r_b(0) = 1.16, r_b'(0) = 0$
3	$\kappa_z(0) = 3.79, \eta = \frac{1}{6}$	45.5°	$r_b(0) = 2.3, r_b'(0) = 0$
5	$\kappa_z(0) = 24.2, \eta = \frac{1}{6}$	115°	$r_b(0) = 1.4, r_b'(0) = 0$

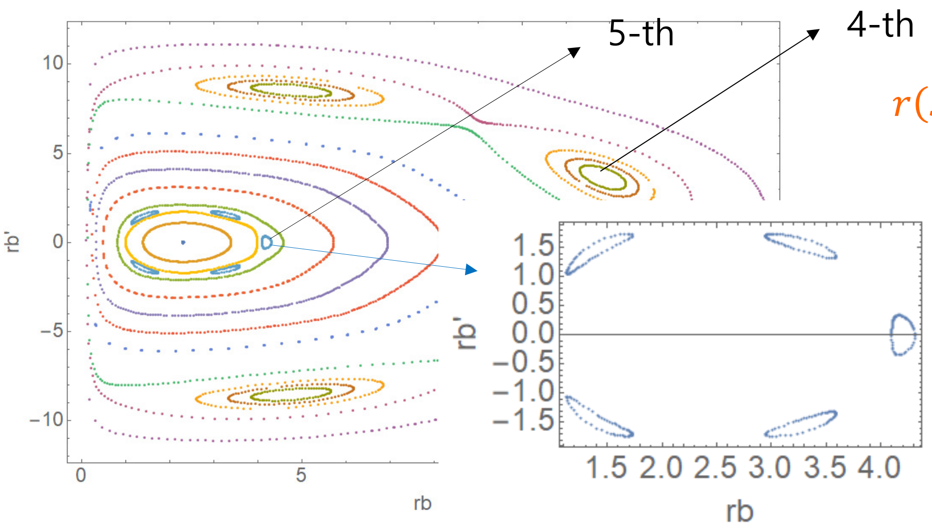

n-th order resonance

$$r(s) = r_b(s; matched) + \delta r \;,\; \delta r(s) = \delta r(0) \boldsymbol{cos(k_n s)}$$

High-intensity charged-particle beam physics

Nonlinear resonances and chaotic motions of envelope oscillation

All points are plotted **in every S lattice period** (Poincare surface of section plots) with different envelope initial conditions for propagation **over 300 lattice periods**

Envelope oscillations

(phase plane r_b -$r_b{}'$)

$$r_b{}''(s) + \kappa_z(s) r_b(s) - \frac{K}{r_b(s)} - \frac{1}{r_b{}^3(s)} = 0$$

Space charge perveance (K)	Focusing field parameter	Vacuum phase advance (σ_0)	Matched beam initial condition
0	$\kappa_z(0) = 3.79$,$\eta = \frac{1}{6}$	45.5°	$\boldsymbol{r_b}(0) = 1.16$,$\boldsymbol{r'_b}(0) = 0$
3	$\kappa_z(0) = 3.79$,$\eta = \frac{1}{6}$	45.5°	$\boldsymbol{r_b}(0) = 2.3$,$\boldsymbol{r'_b}(0) = 0$
5	$\kappa_z(0) = 24.2$,$\eta = \frac{1}{6}$	115°	$\boldsymbol{r_b}(0) = 1.4$,$\boldsymbol{r'_b}(0) = 0$

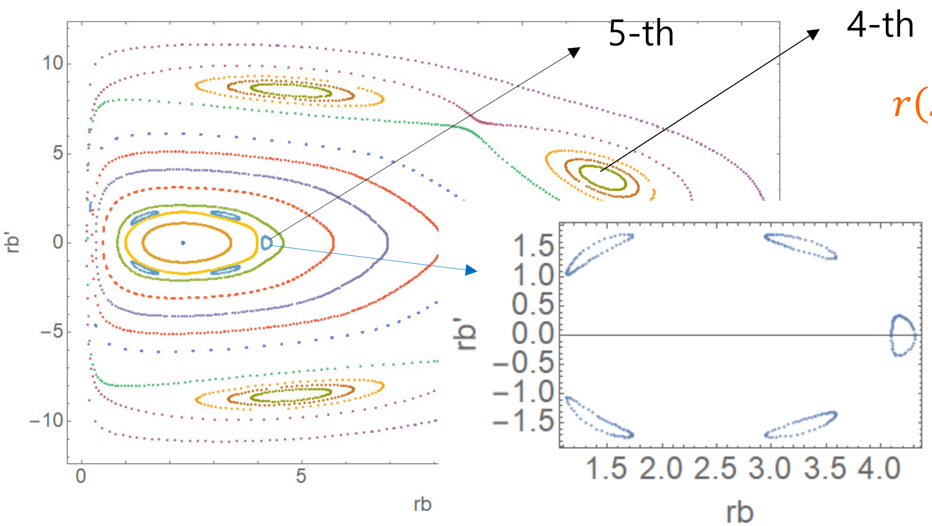

n-th order resonance

$$r(s) = r_b(s; matched) + \delta r \ \ , \ \ \delta r(s) = \delta r(0)\boldsymbol{cos(k_n s)}$$

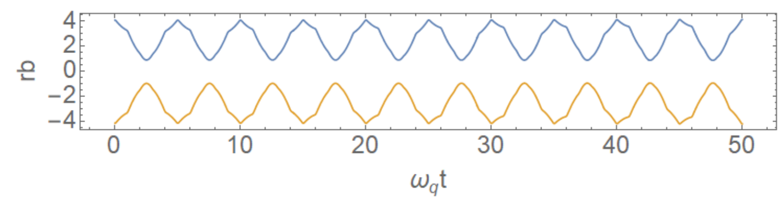

High-intensity charged-particle beam physics

Nonlinear resonances and chaotic motions of envelope oscillation

All points are plotted **in every S lattice period** (Poincare surface of section plots) with different envelope initial conditions for propagation **over 300 lattice periods**

Envelope oscillations

(phase plane r_b -r_b')

$$r_b''(s) + \kappa_z(s) r_b(s) - \frac{K}{r_b(s)} - \frac{1}{{r_b}^3(s)} = 0$$

Space charge perveance (K)	Focusing field parameter	Vacuum phase advance (σ_0)	Matched beam initial condition
0	$\kappa_z(0) = 3.79$,$\eta = \frac{1}{6}$	45.5°	$\boldsymbol{r_b}(0) = 1.16$,$\boldsymbol{r_b'}(0) = 0$
3	$\kappa_z(0) = 3.79$,$\eta = \frac{1}{6}$	45.5°	$\boldsymbol{r_b}(0) = 2.3$,$\boldsymbol{r_b'}(0) = 0$
5	$\kappa_z(0) = 24.2$,$\eta = \frac{1}{6}$	115°	$\boldsymbol{r_b}(0) = 1.4$,$\boldsymbol{r_b'}(0) = 0$

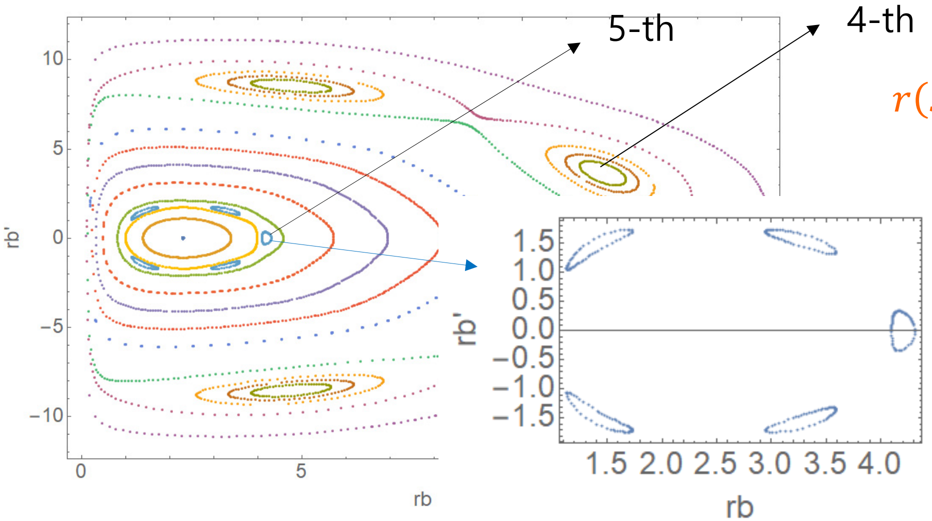

n-th order resonance

$$r(s) = r_b(s; matched) + \delta r \;,\; \delta r(s) = \delta r(0) \boldsymbol{\cos(k_n s)}$$

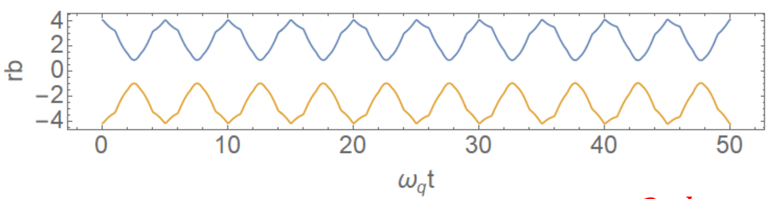

n=5 ; 5-th order resonance $\mathrm{k} = k_5 = \frac{2\pi l}{5}$

if $s = 5, 10, 15, \ldots,$

the perturbed radius comes back its starting point

High-intensity charged-particle beam physics

Nonlinear resonances and chaotic motions of envelope oscillation

All points are plotted **in every S lattice period** (Poincare surface of section plots) with different envelope initial conditions for propagation **over 300 lattice periods**

Envelope oscillations

(phase plane r_b -$r_b{}'$)

$$r_b{}''(s) + \kappa_z(s) r_b(s) - \frac{K}{r_b(s)} - \frac{1}{r_b{}^3(s)} = 0$$

Space charge perveance (K)	Focusing field parameter	Vacuum phase advance (σ_0)	Matched beam initial condition
0	$\kappa_z(0) = 3.79$,$\eta = \frac{1}{6}$	45.5°	$\boldsymbol{r_b}(0) = 1.16$,$\boldsymbol{r'_b}(0) = 0$
3	$\kappa_z(0) = 3.79$,$\eta = \frac{1}{6}$	45.5°	$\boldsymbol{r_b}(0) = 2.3$,$\boldsymbol{r'_b}(0) = 0$
5	$\kappa_z(0) = 24.2$,$\eta = \frac{1}{6}$	115°	$\boldsymbol{r_b}(0) = 1.4$,$\boldsymbol{r'_b}(0) = 0$

High-intensity charged-particle beam physics

Nonlinear resonances and chaotic motions of envelope oscillation

All points are plotted **in every S lattice period** (Poincare surface of section plots) with different envelope initial conditions for propagation **over 300 lattice periods**

Envelope oscillations

(phase plane r_b -r_b')

$$r_b''(s) + \kappa_z(s) r_b(s) - \frac{K}{r_b(s)} - \frac{1}{{r_b}^3(s)} = 0$$

Space charge perveance (K)	Focusing field parameter	Vacuum phase advance (σ_0)	Matched beam initial condition
0	$\kappa_z(0) = 3.79$,$\eta = \frac{1}{6}$	45.5°	$\boldsymbol{r_b}(0) = 1.16$,$\boldsymbol{r'_b}(0) = 0$
3	$\kappa_z(0) = 3.79$,$\eta = \frac{1}{6}$	45.5°	$\boldsymbol{r_b}(0) = 2.3$,$\boldsymbol{r'_b}(0) = 0$
5	$\kappa_z(0) = 24.2$,$\eta = \frac{1}{6}$	115°	$\boldsymbol{r_b}(0) = 1.4$,$\boldsymbol{r'_b}(0) = 0$

High-intensity charged-particle beam physics

Nonlinear resonances and chaotic motions of envelope oscillation

All points are plotted **in every S lattice period** (Poincare surface of section plots) with different envelope initial conditions for propagation **over 300 lattice periods**

Envelope oscillations

(phase plane r_b -r_b')

$$r_b''(s) + \kappa_z(s) r_b(s) - \frac{K}{r_b(s)} - \frac{1}{r_b{}^3(s)} = 0$$

Space charge perveance (K)	Focusing field parameter	Vacuum phase advance (σ_0)	Matched beam initial condition
0	$\kappa_z(0) = 3.79$,$\eta = \frac{1}{6}$	45.5°	$\boldsymbol{r_b}(0) = 1.16$,$\boldsymbol{r'_b}(0) = 0$
3	$\kappa_z(0) = 3.79$,$\eta = \frac{1}{6}$	45.5°	$\boldsymbol{r_b}(0) = 2.3$,$\boldsymbol{r'_b}(0) = 0$
5	$\kappa_z(0) = 24.2$,$\eta = \frac{1}{6}$	115°	$\boldsymbol{r_b}(0) = 1.4$,$\boldsymbol{r'_b}(0) = 0$

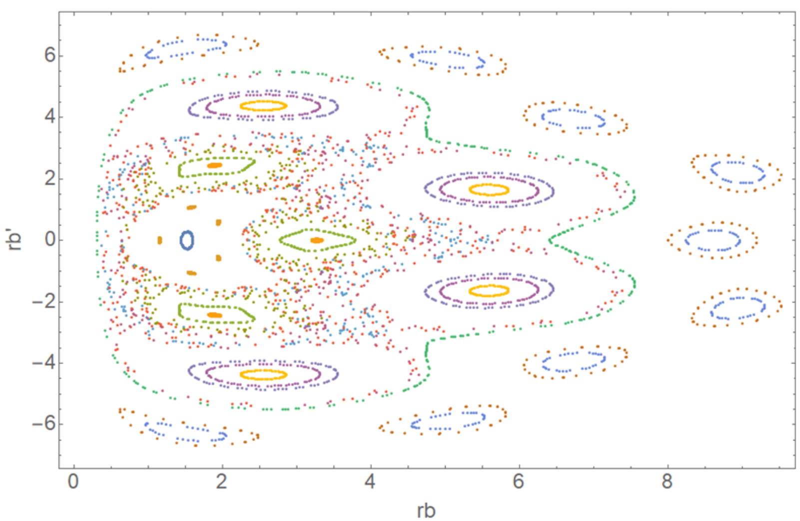

Contents

Halo formation of transverse particle-core model

Halo formations of particles along the linac

Halo formation of transverse particle-core model

Halo formations of particles along the linac

Halo formation of transverse particle-core model

Halo formations of particles along the linac

→ Beam emittance growth and particle losses in accelerators

Halo formation of transverse particle-core model

Halo formations of particles along the linac

→ Beam emittance growth and particle losses in accelerators →

Halo formation of transverse particle-core model

Halo formations of particles along the linac

→ Beam emittance growth and particle losses in accelerators → Radioactivation

Halo formation of transverse particle-core model

Halo formations of particles along the linac

→ Beam emittance growth and particle losses in accelerators → Radioactivation

- Uniform charge density

Halo formation of transverse particle-core model

Halo formations of particles along the linac

→ Beam emittance growth and particle losses in accelerators → Radioactivation

- Uniform charge density

<table>
<tr><td rowspan="3">Envelope</td><td>Matched</td><td>Beam core oscillates periodically in every lattice period</td><td></td></tr>
<tr><td>Mis-matched</td><td rowspan="2">Beam core oscillates because of initial mismatch
&
Space charge effect</td><td>Envelope oscillation</td></tr>
<tr><td>n-th order resonance</td><td>Particle frequency</td></tr>
</table>

Halo formation of transverse particle-core model

Halo formations of particles along the linac

→ Beam emittance growth and particle losses in accelerators → Radioactivation

- Uniform charge density

Envelope	Matched	Beam core oscillates periodically in every lattice period	
	Mis-matched	Beam core oscillates because of initial mismatch & Space charge effect	Envelope oscillation **Resonance** Particle frequency
	n-th order resonance		

Halo formation of transverse particle-core model

Halo formations of particles along the linac

→ Beam emittance growth and particle losses in accelerators → Radioactivation

- Uniform charge density

Envelope	Matched	Beam core oscillates periodically in every lattice period	
	Mis-matched	Beam core oscillates because of initial mismatch & Space charge effect	Envelope oscillation ↕ **Resonance** ↕ Particle frequency
	n-th order resonance		

- Non-uniform charge density (**Gaussian**)

Halo formation of transverse particle-core model

Halo formations of particles along the linac

→ Beam emittance growth and particle losses in accelerators → Radioactivation

- Uniform charge density

<table>
<tr><td rowspan="3">Envelope</td><td>Matched</td><td>Beam core oscillates periodically in every lattice period</td><td></td></tr>
<tr><td>Mis-matched</td><td rowspan="2">Beam core oscillates because of initial mismatch
&
Space charge effect</td><td rowspan="2">Envelope oscillation
↕ Resonance
Particle frequency</td></tr>
<tr><td>n-th order resonance</td></tr>
</table>

- Non-uniform charge density (**Gaussian**)

Envelope	Matched	Gaussian density profile	**Non-linear space charge force**

Halo formation of transverse particle-core model

Halo formations of particles along the linac

→ Beam emittance growth and particle losses in accelerators → Radioactivation

- External : **periodic solenoidal magnetic focusing field**
- Uniform charge density

Envelope	Matched	Beam core oscillates periodically in every lattice period	
	Mis-matched	Beam core oscillates because of initial mismatch & Space charge effect	Envelope oscillation ↕ **Resonance** ↕ Particle frequency
	n-th order resonance		

- Non-uniform charge density (**Gaussian**)

Envelope	Matched	Gaussian density profile	**Non-linear space charge force**

Halo formation of transverse particle-core model

Uniform density charged particle motions

Halo formation of transverse particle-core model

Uniform density charged particle motions

Equation of motion (Larmor frame)

Halo formation of transverse particle-core model

Uniform density charged particle motions

Equation of motion (Larmor frame)

$$\boldsymbol{x''(s) + \kappa_z(s)x(s) - KF(x, r_b) = 0}$$

$F(x, r_b) = \frac{x(s)}{{r_b}^2(s)}$ for $x(s) < r_b(s)$, $\frac{1}{x(s)}$ for $x(s) > r_b(s)$

Halo formation of transverse particle-core model

Uniform density charged particle motions

Equation of motion (Larmor frame)

(phase plane x/r_b-x')

$$\boldsymbol{x''(s) + \kappa_z(s)x(s) - KF(x, r_b) = 0}$$

$F(x, r_b) = \frac{x(s)}{{r_b}^2(s)}$ for $x(s) < r_b(s)$, $\frac{1}{x(s)}$ for $x(s) > r_b(s)$

Halo formation of transverse particle-core model

All points are plotted **in every S lattice period** (Poincare surface of section plots) with different particle initial conditions for propagation **over 300 lattice periods**

Uniform density charged particle motions

Equation of motion (Larmor frame)

(phase plane x/r_b-x')

$$\boldsymbol{x''(s) + \kappa_z(s)x(s) - KF(x, r_b) = 0}$$

$$F(x, r_b) = \frac{x(s)}{{r_b}^2(s)} \text{ for } x(s) < r_b(s), \quad \frac{1}{x(s)} \text{ for } x(s) > r_b(s)$$

Halo formation of transverse particle-core model

All points are plotted **in every S lattice period** (Poincare surface of section plots) with different particle initial conditions for propagation **over 300 lattice periods**

Uniform density charged particle motions

Equation of motion (Larmor frame)

(phase plane x/r_b-x')

$$x''(s) + \kappa_z(s)x(s) - KF(x, r_b) = 0$$

$$F(x, r_b) = \frac{x(s)}{{r_b}^2(s)} \text{ for } x(s) < r_b(s), \quad \frac{1}{x(s)} \text{ for } x(s) > r_b(s)$$

Matched core – test particles

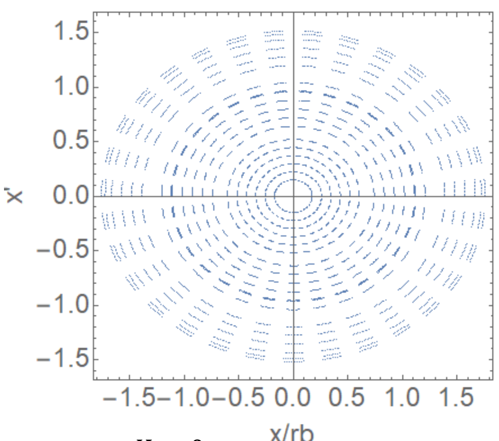

$K = 0$

$\sigma_0 = 45.5^\circ$

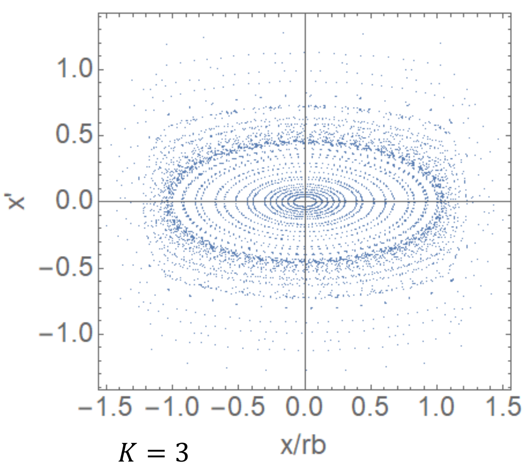

$K = 3$

$\sigma_0 = 45.5^\circ$

Halo formation of transverse particle-core model

All points are plotted **in every S lattice period** (Poincare surface of section plots) with different particle initial conditions for propagation **over 300 lattice periods**

Uniform density charged particle motions

Equation of motion (Larmor frame)

(phase plane x/r_b-x')

$$\boldsymbol{x''(s) + \kappa_z(s)x(s) - KF(x, r_b) = 0}$$

$$F(x, r_b) = \frac{x(s)}{{r_b}^2(s)} \text{ for } x(s) < r_b(s), \quad \frac{1}{x(s)} \text{ for } x(s) > r_b(s)$$

Matched core – test particles

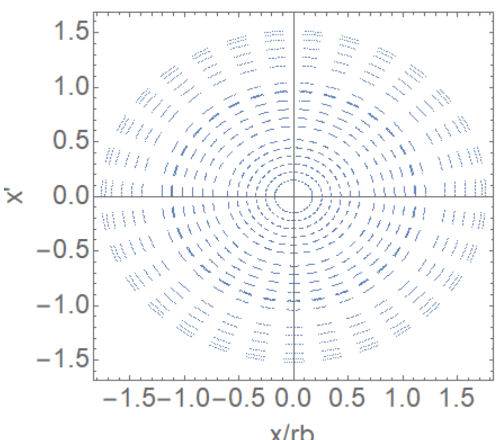

$K = 0$

$\sigma_0 = 45.5^{\circ}$

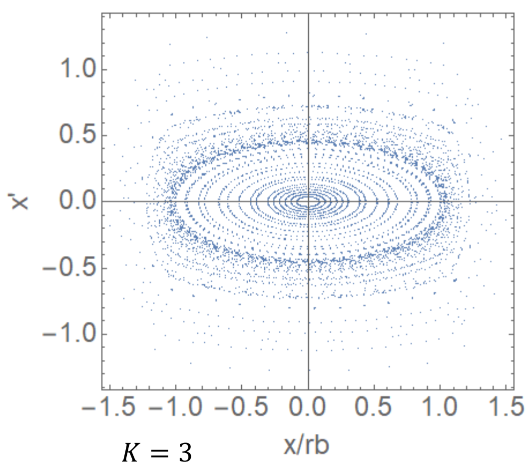

$K = 3$

$\sigma_0 = 45.5^{\circ}$

Mismatched core – test particles

$K = 3$

$\sigma_0 = 45.5^{\circ}$

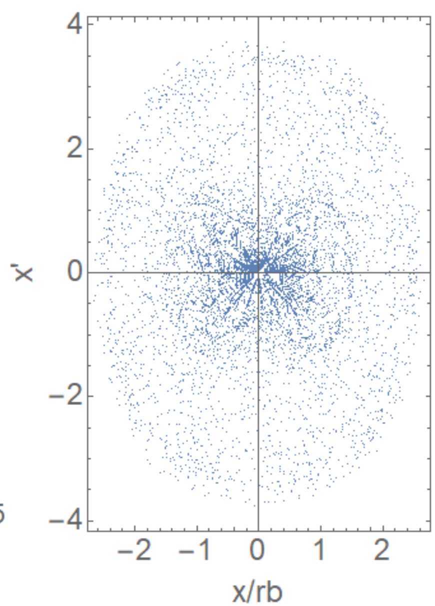

Halo formation of transverse particle-core model

All points are plotted **in every S lattice period** (Poincare surface of section plots) with different particle initial conditions for propagation **over 300 lattice periods**

Uniform density charged particle motions

Equation of motion (Larmor frame)

(phase plane x/r_b-x')

$$\boldsymbol{x''(s) + \kappa_z(s)x(s) - KF(x, r_b) = 0}$$

$$F(x, r_b) = \frac{x(s)}{{r_b}^2(s)} \text{ for } x(s) < r_b(s), \quad \frac{1}{x(s)} \text{ for } x(s) > r_b(s)$$

Matched core – test particles

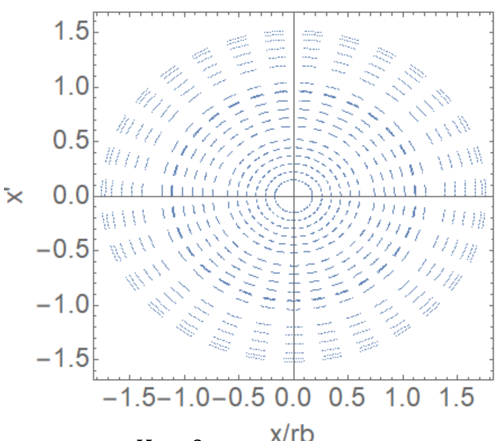

$K = 0$

$\sigma_0 = 45.5^{\circ}$

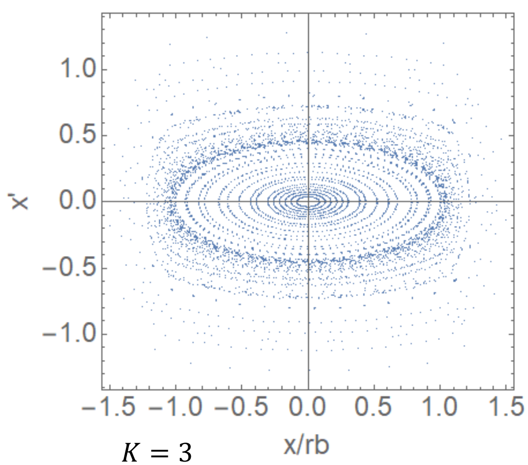

$K = 3$

$\sigma_0 = 45.5^{\circ}$

Mismatched core – test particles

$K = 3$

$\sigma_0 = 45.5^{\circ}$

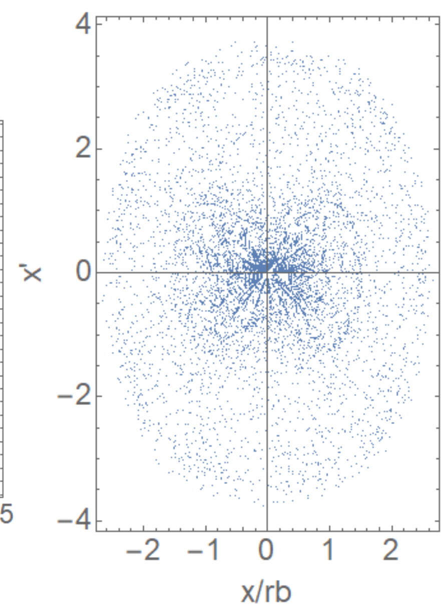

5th resonance core – test particles **(plot in every 5 period)**

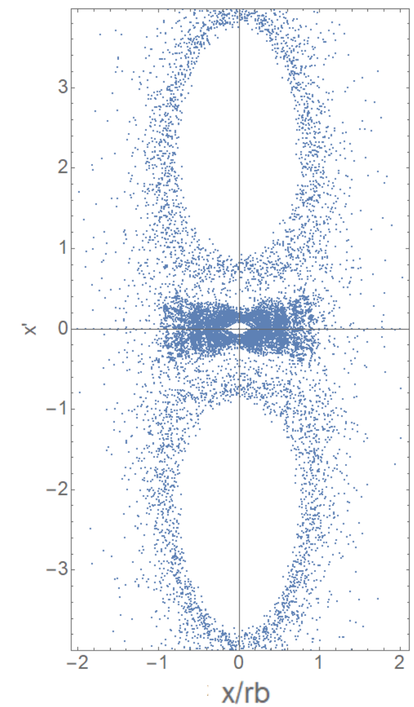

Halo formation of transverse particle-core model

Gaussian density charged particle motions of matched beam

Halo formation of transverse particle-core model

Gaussian density charged particle motions of matched beam

Space charge field of gaussian density particles

Halo formation of transverse particle-core model

Gaussian density charged particle motions of matched beam

Space charge field of gaussian density particles

For Gaussian charge density,

$$\rho(\mathrm{x}) = \frac{\lambda}{2\pi\sigma_x\sigma_y}\exp\left(-\frac{x^2}{2\sigma_x^2} - \frac{y^2}{2\sigma_y^2}\right)$$

$$\boldsymbol{E_{sc,x}(x,y) = 2\lambda\frac{1-e^{-r^2/\sigma_r^2}}{r^2}x} \ , \qquad \boldsymbol{E_{sc,y}(x,y) = 2\lambda\frac{1-e^{-r^2/\sigma_r^2}}{r^2}y}$$

$$r^2 = x^2 + y^2$$

Halo formation of transverse particle-core model

Gaussian density charged particle motions of matched beam

Space charge field of gaussian density particles

For Gaussian charge density,

$$\rho(\mathrm{x}) = \frac{\lambda}{2\pi\sigma_x\sigma_y}\exp\left(-\frac{x^2}{2\sigma_x^2}-\frac{y^2}{2\sigma_y^2}\right)$$

$$\boldsymbol{E_{sc,x}(x,y) = 2\lambda\frac{1-e^{-r^2/\sigma_r^2}}{r^2}x} \ , \qquad \boldsymbol{E_{sc,y}(x,y) = 2\lambda\frac{1-e^{-r^2/\sigma_r^2}}{r^2}y}$$

$$r^2 = x^2 + y^2$$

For symmetric case, $\sigma_r = \sqrt{2}\sigma_x = \sqrt{2}\sigma_y$

$$\rho(r) = \frac{\lambda}{\pi{\sigma_r}^2}\exp(-\frac{r^2}{{\sigma_r}^2})$$

$$\boldsymbol{E_{sc,r}(r) = 2\lambda\frac{1-e^{-r^2/\sigma_r^2}}{r}}$$

Halo formation of transverse particle-core model

Gaussian density charged particle motions of matched beam

Space charge field of gaussian density particles

For Gaussian charge density,

$$\rho(\mathrm{x}) = \frac{\lambda}{2\pi\sigma_x\sigma_y}\exp\left(-\frac{x^2}{2\sigma_x^2} - \frac{y^2}{2\sigma_y^2}\right)$$

$$\boldsymbol{E_{sc,x}(x,y) = 2\lambda\frac{1-e^{-r^2/\sigma_r^2}}{r^2}x}\ , \qquad \boldsymbol{E_{sc,y}(x,y) = 2\lambda\frac{1-e^{-r^2/\sigma_r^2}}{r^2}y}$$

$$r^2 = x^2 + y^2$$

For symmetric case, $\sigma_r = \sqrt{2}\sigma_x = \sqrt{2}\sigma_y$

$$\rho(r) = \frac{\lambda}{\pi{\sigma_r}^2}\exp(-\frac{r^2}{{\sigma_r}^2})$$

$$\boldsymbol{\sigma_r(s) = r_b/\sqrt{2}}$$

(equivalent beams)

$$\boldsymbol{E_{sc,r}(r) = 2\lambda\frac{1-e^{-r^2/\sigma_r^2}}{r}}$$

Halo formation of transverse particle-core model

Gaussian density charged particle motions of matched beam

Space charge field of gaussian density particles

For Gaussian charge density,

$$\rho(\mathrm{x}) = \frac{\lambda}{2\pi\sigma_x\sigma_y}\exp\left(-\frac{x^2}{2\sigma_x^2}-\frac{y^2}{2\sigma_y^2}\right)$$

$$\boldsymbol{E_{sc,x}(x,y) = 2\lambda\frac{1-e^{-r^2/\sigma_r^2}}{r^2}x}\ ,\qquad \boldsymbol{E_{sc,y}(x,y) = 2\lambda\frac{1-e^{-r^2/\sigma_r^2}}{r^2}y}$$

$$r^2 = x^2 + y^2$$

For symmetric case, $\sigma_r = \sqrt{2}\sigma_x = \sqrt{2}\sigma_y$

$$\rho(r) = \frac{\lambda}{\pi{\sigma_r}^2}\exp(-\frac{r^2}{{\sigma_r}^2})$$

$$\boldsymbol{E_{sc,r}(r) = 2\lambda\frac{1-e^{-r^2/\sigma_r^2}}{r}}$$

$$\boldsymbol{\sigma_r(s) = r_b/\sqrt{2}}$$

(equivalent beams)

Equation of motion (real frame)

Coupled equation of motion

$$\begin{cases} x''(s) - 2\sqrt{\kappa_z(s)}y'(s) - \frac{K}{2}F_{sc,x}(x,y) = 0 \\ y''(s) + 2\sqrt{\kappa_z(s)}x'(s) - \frac{K}{2}F_{sc,y}(x,y) = 0 \end{cases}$$

$$F_{sc,x}(x,y) = 2\frac{1-e^{-r^2/\sigma_r^2}}{r^2}x$$

$$F_{sc,y}(x,y) = 2\frac{1-e^{-r^2/\sigma_r^2}}{r^2}y$$

When $p_\theta \neq 0\ ,\quad \gamma' = \gamma'' = 0$

Halo formation of transverse particle-core model

Gaussian density charged particle motions of matched beam

Space charge field of gaussian density particles

For Gaussian charge density,

$$\rho(\mathrm{x}) = \frac{\lambda}{2\pi\sigma_x\sigma_y}\exp\left(-\frac{x^2}{2\sigma_x^2}-\frac{y^2}{2\sigma_y^2}\right)$$

$$\boldsymbol{E_{sc,x}(x,y) = 2\lambda\frac{1-e^{-r^2/\sigma_r^2}}{r^2}x}\ , \qquad \boldsymbol{E_{sc,y}(x,y) = 2\lambda\frac{1-e^{-r^2/\sigma_r^2}}{r^2}y}$$

$$r^2 = x^2 + y^2$$

For symmetric case, $\sigma_r = \sqrt{2}\sigma_x = \sqrt{2}\sigma_y$

$$\rho(r) = \frac{\lambda}{\pi{\sigma_r}^2}\exp\left(-\frac{r^2}{{\sigma_r}^2}\right)$$

$$\boldsymbol{\sigma_r(s) = r_b/\sqrt{2}}$$

(equivalent beams)

$$\boldsymbol{E_{sc,r}(r) = 2\lambda\frac{1-e^{-r^2/\sigma_r^2}}{r}}$$

Equation of motion (real frame)

Coupled equation of motion

$$\begin{cases} x''(s) - 2\sqrt{\kappa_z(s)}y'(s) - \frac{K}{2}F_{sc,x}(x,y) = 0 \\ y''(s) + 2\sqrt{\kappa_z(s)}x'(s) - \frac{K}{2}F_{sc,y}(x,y) = 0 \end{cases}$$

$$F_{sc,x}(x,y) = 2\frac{1-e^{-r^2/\sigma_r^2}}{r^2}x$$

$$F_{sc,y}(x,y) = 2\frac{1-e^{-r^2/\sigma_r^2}}{r^2}y$$

When $p_\theta \neq 0$, $\gamma' = \gamma'' = 0$

Radial equation of motion (real frame)

$$r''(s) + \kappa_z(s)r(s) - \frac{K}{2}F_{sc}(r) = 0$$

$$F_{sc}(r) = 2\frac{1-e^{-r^2/\sigma_r^2}}{r}$$

When $p_\theta = 0$; $y = y' = 0$, $\gamma' = \gamma'' = 0$

Halo formation of transverse particle-core model

All points are plotted **in every S lattice period** (Poincare surface of section plots) with different particle initial conditions for propagation **over 300 lattice periods**

Gaussian density charged particle motions of matched beam

Transverse particle motions (real frame)

Radial equation of motion

(phase plane r/r_b-r')

$$r''(s) + \kappa_z(s) r(s) - \frac{K}{2} F_{sc}(r) = 0$$

$$F_{sc}(r) = 2\frac{1 - e^{-r^2/\sigma_r^2}}{r}$$

Halo formation of transverse particle-core model

Gaussian density charged particle motions of matched beam

Transverse particle motions (real frame)

Radial equation of motion

(phase plane r/r_b-r′)

$$r''(s) + \kappa_z(s)r(s) - \frac{K}{2}F_{sc}(r) = 0$$

$$F_{sc}(r) = 2\frac{1 - e^{-r^2/\sigma_r^2}}{r}$$

K=0 , $\sigma_0 = 45.5°$, $\sigma = 46°$

$$\frac{\sigma}{\sigma_0} = 1$$

All points are plotted **in every S lattice**

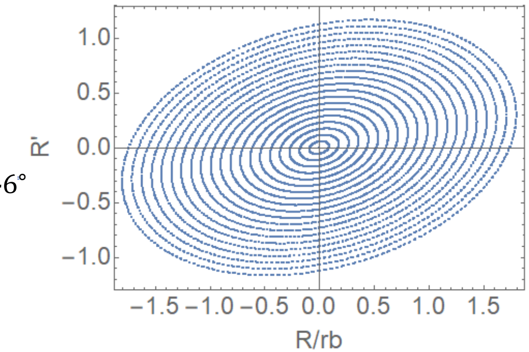

Halo formation of transverse particle-core model

All points are plotted **in every S lattice**

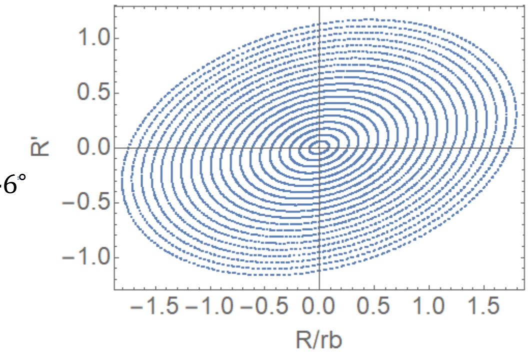

K=0 , $\sigma_0 = 45.5°$, $\sigma = 46°$

$$\frac{\sigma}{\sigma_0} = 1$$

Gaussian density charged particle motions of matched beam

Transverse particle motions (real frame)

Radial equation of motion

(phase plane r/r_b-r′)

$$r''(s) + \kappa_z(s) r(s) - \frac{K}{2} F_{sc}(r) = 0$$

$$F_{sc}(r) = 2\frac{1 - e^{-r^2/\sigma_r^2}}{r}$$

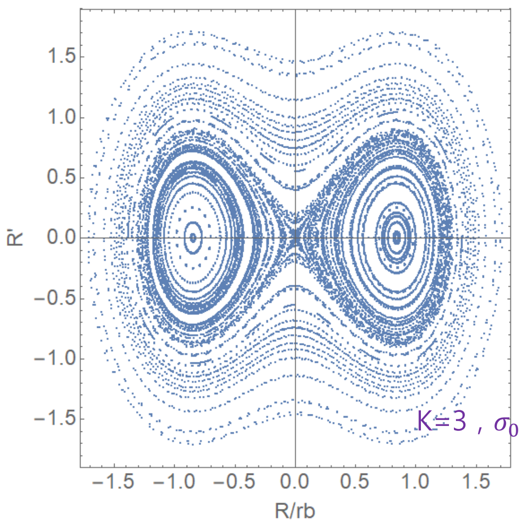

K=3 , $\sigma_0 = 45.5°$, $\sigma = 12°$

$$\frac{\sigma}{\sigma_0} = 0.26$$

Halo formation of transverse particle-core model

All points are plotted in every S lattice

Gaussian density charged particle motions of matched beam

Transverse particle motions (real frame)

Radial equation of motion

(phase plane r/r_b-r′)

$$r''(s) + \kappa_z(s) r(s) - \frac{K}{2} F_{sc}(r) = 0$$

$$F_{sc}(r) = 2\frac{1 - e^{-r^2/\sigma_r^2}}{r}$$

K=0 , $\sigma_0 = 45.5° , \sigma = 46°$ $\frac{\sigma}{\sigma_0} = 1$

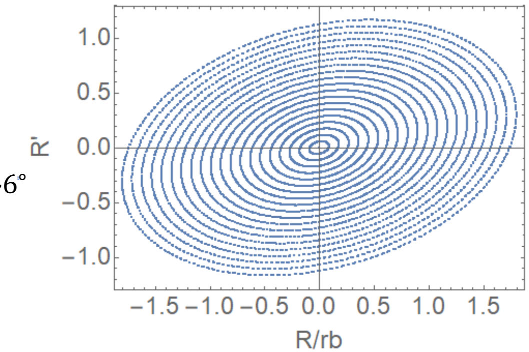

K=4.7 , $\sigma_0 = 130° , \sigma = 60°$ $\frac{\sigma}{\sigma_0} = 0.46$

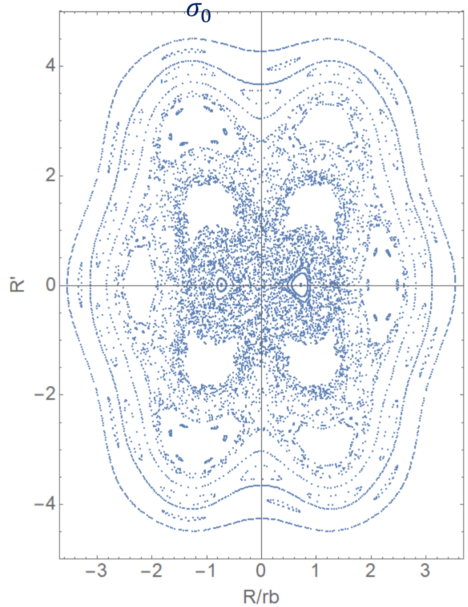

K=2.3 , $\sigma_0 = 115° , \sigma = 90°$ $\frac{\sigma}{\sigma_0} = 0.78$

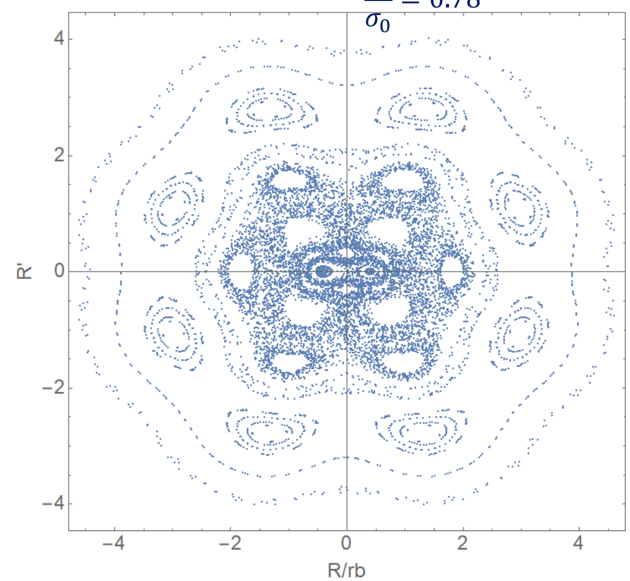

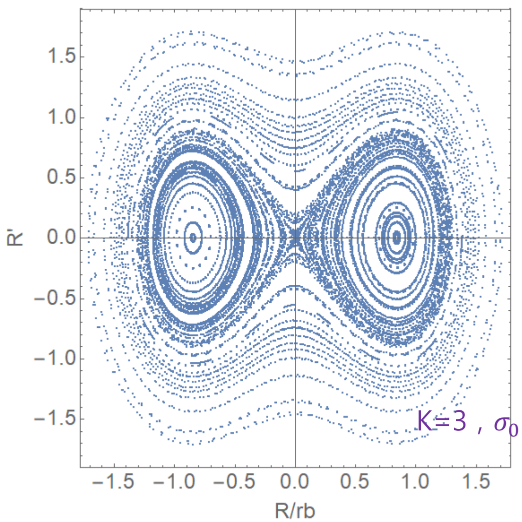

K=3 , $\sigma_0 = 45.5° , \sigma = 12°$ $\frac{\sigma}{\sigma_0} = 0.26$

Halo formation of transverse particle-core model

Gaussian density charged particle motions of matched beam

Transverse particle motions (real frame)

Radial equation of motion

$$r''(s) + \kappa_z(s)r(s) - \frac{K}{2}F_{sc}(r) = 0$$

$$F_{sc}(r) = 2\frac{1 - e^{-r^2/\sigma_r^2}}{r}$$

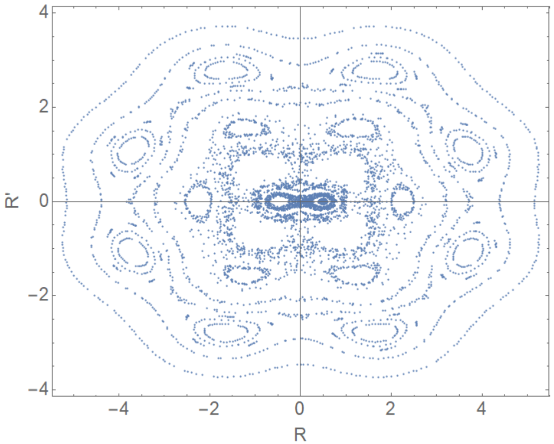

K=2.3 , $\sigma_0 = 115°$, $\boldsymbol{\sigma = 90°}$

Halo formation of transverse particle-core model

Gaussian density charged particle motions of matched beam

Transverse particle motions (real frame)

Radial equation of motion

$$r''(s) + \kappa_z(s) r(s) - \frac{K}{2} F_{sc}(r) = 0$$

$$F_{sc}(r) = 2\frac{1 - e^{-r^2/\sigma_r^2}}{r} \quad \rightarrow \quad e^{-r^2/\sigma_r^2} = \sum_{n=0}^{\infty} \frac{1}{n!}\left(-\frac{r^2}{\sigma_r^2}\right)^n$$

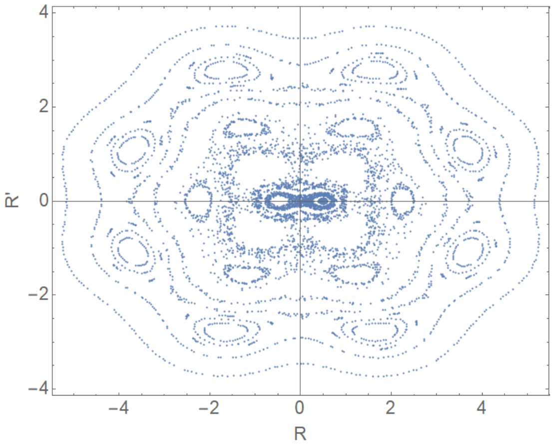

K=2.3 , $\sigma_0 = 115°$, $\boldsymbol{\sigma = 90°}$

Halo formation of transverse particle-core model

Gaussian density charged particle motions of matched beam

Transverse particle motions (real frame)

Radial equation of motion

$$r''(s) + \kappa_z(s) r(s) - \frac{K}{2} F_{sc}(r) = 0$$

With n≤2 ; n=1 (linear), n=2 (2nd order)

-> $r''(s) + {\sigma_\perp}^2 r(s) \sim r^3 \cdot e^{i\sigma_{env} s}$ **;** $r \sim e^{\pm i \sigma_\perp s}$

< Resonance condition >

-> $\sigma_{env} = 4\sigma_\perp$ **;** $\sigma_{env} = 360°$ (matched beam)

-> $\boldsymbol{\sigma_\perp = 90° : 4^{th} order\ resonance}$

$$F_{sc}(r) = 2\frac{1 - e^{-r^2/\sigma_r^2}}{r}$$

$$e^{-r^2/\sigma_r^2} = \sum_{n=0}^{\infty} \frac{1}{n!}\left(-\frac{r^2}{\sigma_r^2}\right)^n$$

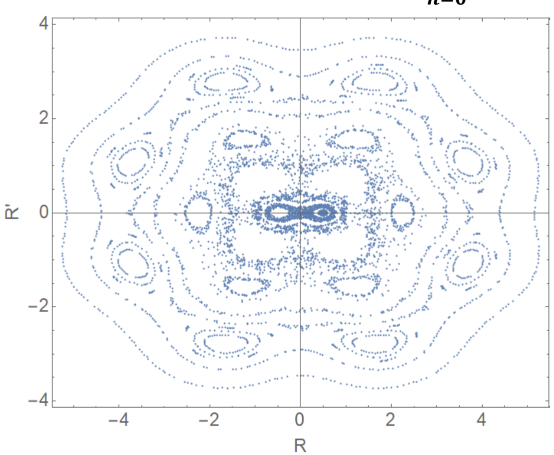

K=2.3 , $\sigma_0 = 115°$, $\boldsymbol{\sigma = 90°}$

Halo formation of transverse particle-core model

Gaussian density charged particle motions of matched beam

Transverse particle motions (real frame)

Radial equation of motion

$$r''(s) + \kappa_z(s)r(s) - \frac{K}{2}F_{sc}(r) = 0$$

$$F_{sc}(r) = 2\frac{1 - e^{-r^2/\sigma_r^2}}{r}$$

$$e^{-r^2/\sigma_r^2} = \sum_{n=0}^{\infty}\frac{1}{n!}\left(-\frac{r^2}{\sigma_r^2}\right)^n$$

With n≤2 ; n=1 (linear), n=2 (2nd order)

-> $r''(s) + {\sigma_\perp}^2 r(s) \sim r^3 \cdot e^{i\sigma_{env}s}$; $r \sim e^{\pm i\sigma_\perp s}$

< Resonance condition >

-> $\sigma_{env} = 4\sigma_\perp$; $\sigma_{env} = 360°$ (matched beam)

-> $\boldsymbol{\sigma_\perp = 90°}$: $\boldsymbol{4^{th} order\ resonance}$

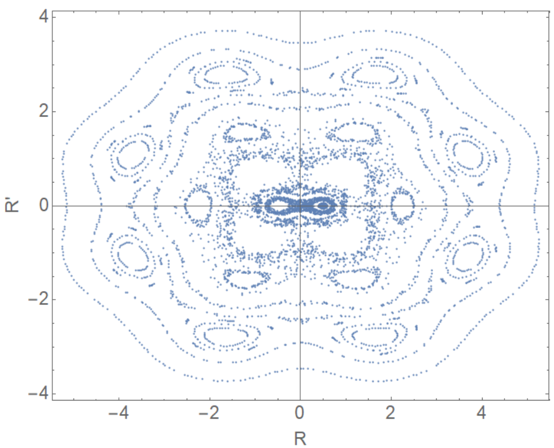

K=2.3 , $\sigma_0 = 115°$, $\boldsymbol{\sigma = 90°}$

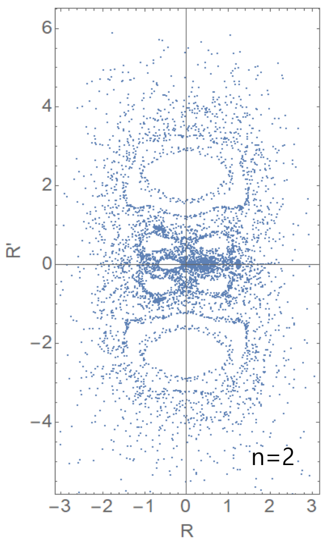

Halo formation of transverse particle-core model

Gaussian density charged particle motions of matched beam

Transverse particle motions (real frame)

Radial equation of motion

$$r''(s) + \kappa_z(s) r(s) - \frac{K}{2} F_{sc}(r) = 0$$

$$F_{sc}(r) = 2\frac{1 - e^{-r^2/\sigma_r^2}}{r} \qquad e^{-r^2/\sigma_r^2} = \sum_{n=0}^{\infty} \frac{1}{n!}\left(-\frac{r^2}{\sigma_r^2}\right)^n$$

With n≤2 ; n=1 (linear), n=2 (2^{nd} order)
-> $r''(s) + \sigma_\perp{}^2 r(s) \sim r^3 \cdot e^{i\sigma_{env}s}$; $r \sim e^{\pm i\sigma_\perp s}$

< Resonance condition >
-> $\sigma_{env} = 4\sigma_\perp$; $\sigma_{env} = 360°$ (matched beam)
-> $\boldsymbol{\sigma_\perp = 90°}$ **: 4^{th} order resonance**

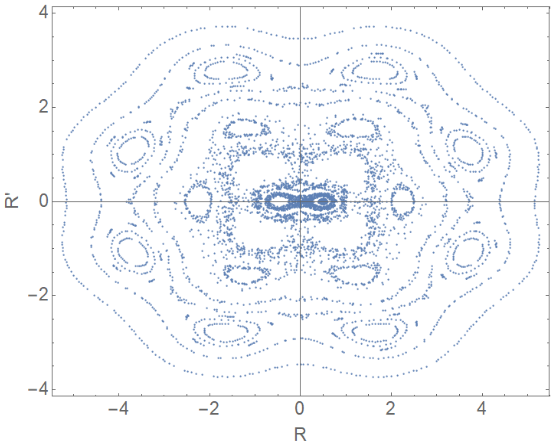

K=2.3 , $\sigma_0 = 115°$, $\boldsymbol{\sigma = 90°}$

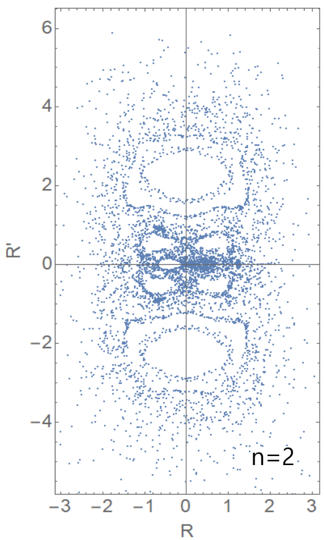

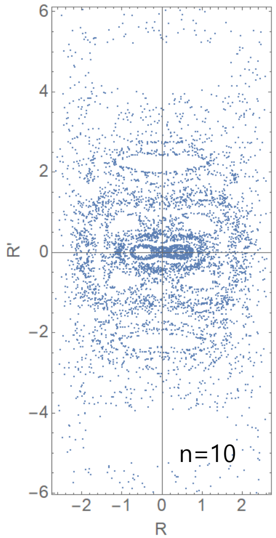

Halo formation of transverse particle-core model

Gaussian density charged particle motions of matched beam

Transverse particle motions (real frame)

Radial equation of motion

$$r''(s) + \kappa_z(s)r(s) - \frac{K}{2}F_{sc}(r) = 0$$

$$F_{sc}(r) = 2\frac{1 - e^{-r^2/\sigma_r^2}}{r} \qquad e^{-r^2/\sigma_r^2} = \sum_{n=0}^{\infty} \frac{1}{n!}\left(-\frac{r^2}{\sigma_r^2}\right)^n$$

With n≤2 ; n=1 (linear), n=2 (2nd order)

-> $r''(s) + {\sigma_\perp}^2 r(s) \sim r^3 \cdot e^{i\sigma_{env}s}$; $r \sim e^{\pm i\sigma_\perp s}$

< Resonance condition >

-> $\sigma_{env} = 4\sigma_\perp$; $\sigma_{env} = 360°$ (matched beam)

-> $\boldsymbol{\sigma_\perp = 90°}$ **: 4^{th} order resonance**

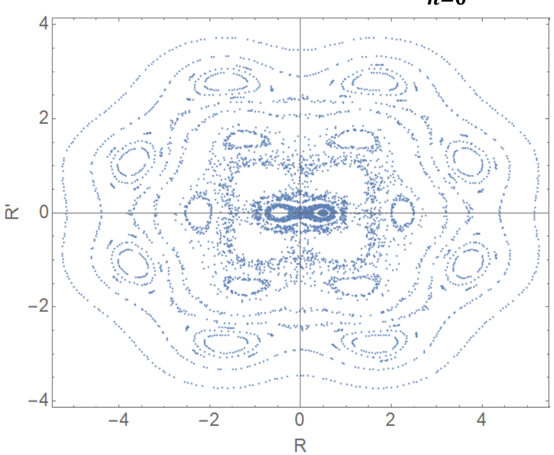

K=2.3 , $\sigma_0 = 115°$, $\boldsymbol{\sigma = 90°}$

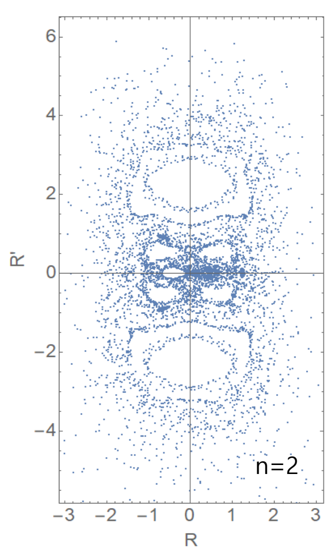

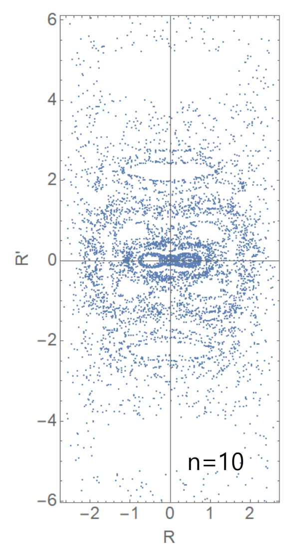

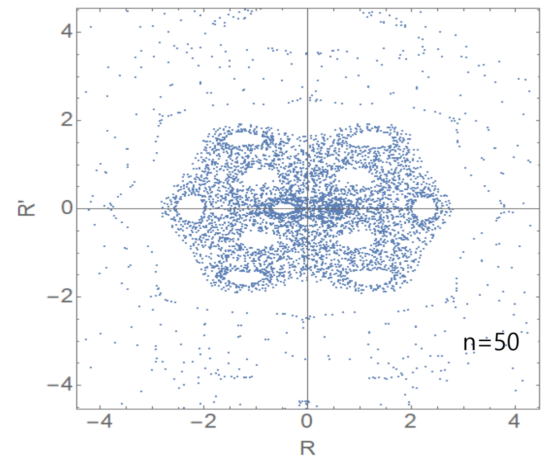

Halo formation of transverse particle-core model

Gaussian density charged particle motions of matched beam

Transverse particle motions (real frame)

Radial equation of motion

$$r''(s) + \kappa_z(s) r(s) - \frac{K}{2} F_{sc}(r) = 0$$

$$F_{sc}(r) = 2\frac{1 - e^{-r^2/\sigma_r^2}}{r}$$

$$e^{-r^2/\sigma_r^2} = \sum_{n=0}^{\infty} \frac{1}{n!}\left(-\frac{r^2}{\sigma_r^2}\right)^n$$

With n≤2 ; n=1 (linear), n=2 (2nd order)

-> $r''(s) + \sigma_\perp{}^2 r(s) \sim r^3 \cdot e^{i\sigma_{env}s}$; $r \sim e^{\pm i\sigma_\perp s}$

< Resonance condition >

-> $\sigma_{env} = 4\sigma_\perp$; $\sigma_{env} = 360°$ (matched beam)

-> $\boldsymbol{\sigma_\perp = 90°}$: ***4^{th} order resonance***

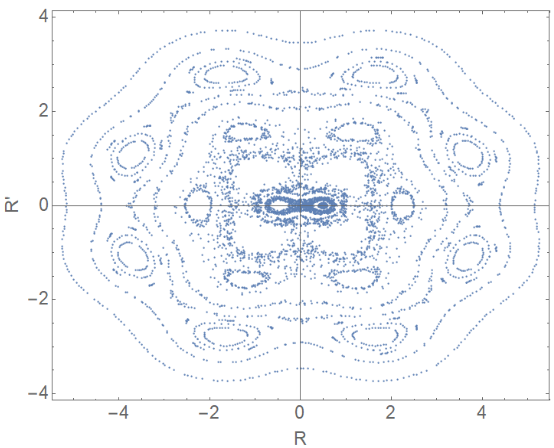

K=2.3 , $\sigma_0 = 115°$, $\boldsymbol{\sigma = 90°}$

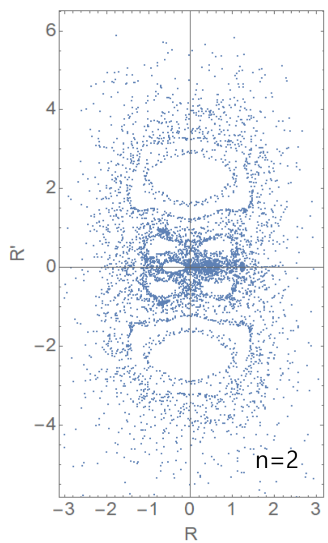

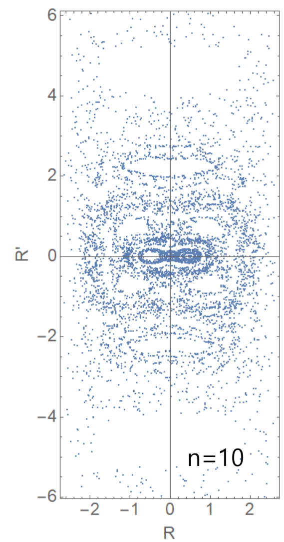

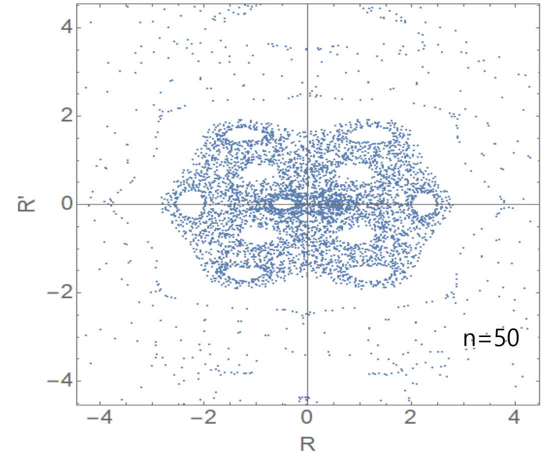

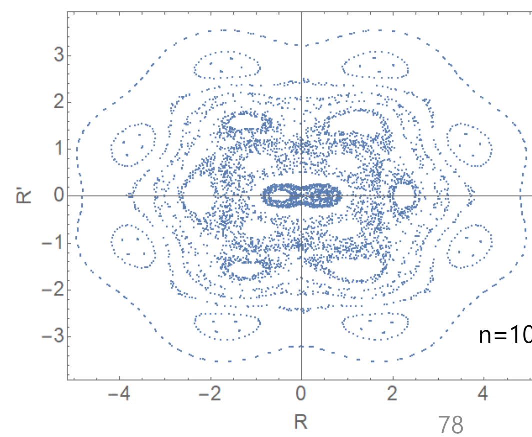

Halo formation of transverse particle-core model

Gaussian density charged particle motions of matched beam

All points are plotted **in every S lattice period** (Poincare surface of section plots) with different particle initial conditions for propagation **over 300 lattice periods**

Transverse particle motions (real frame)

Coupled equation of motion

$$\begin{cases} x''(s) - 2\sqrt{\kappa_z(s)}\,y'(s) - \frac{K}{2}F_{sc,x}(x,y) = 0 \\ y''(s) + 2\sqrt{\kappa_z(s)}\,x'(s) - \frac{K}{2}F_{sc,y}(x,y) = 0 \end{cases}$$

$$F_{sc,x}(x,y) = 2\frac{1-e^{-r^2/\sigma_r^2}}{r^2}x$$

$$F_{sc,y}(x,y) = 2\frac{1-e^{-r^2/\sigma_r^2}}{r^2}y$$

Halo formation of transverse particle-core model

Gaussian density charged particle motions of matched beam

All points are plotted **in every S lattice period** (Poincare surface of section plots) with different particle initial conditions for propagation **over 300 lattice periods**

Transverse particle motions (real frame)

Coupled equation of motion

$$\begin{cases} x''(s) - 2\sqrt{\kappa_z(s)}\,y'(s) - \frac{K}{2}F_{sc,x}(x,y) = 0 \\ y''(s) + 2\sqrt{\kappa_z(s)}\,x'(s) - \frac{K}{2}F_{sc,y}(x,y) = 0 \end{cases}$$

$$F_{sc,x}(x,y) = 2\frac{1-e^{-r^2/\sigma_r^2}}{r^2}x$$

$$F_{sc,y}(x,y) = 2\frac{1-e^{-r^2/\sigma_r^2}}{r^2}y$$

Many test particles with different initial conditions

Halo formation of transverse particle-core model

Gaussian density charged particle motions of matched beam

All points are plotted **in every S lattice period** (Poincare surface of section plots) with different particle initial conditions for propagation **over 300 lattice periods**

Transverse particle motions (real frame)

Coupled equation of motion

$$\begin{cases} x''(s) - 2\sqrt{\kappa_z(s)}\,y'(s) - \frac{K}{2}F_{sc,x}(x,y) = 0 \\ y''(s) + 2\sqrt{\kappa_z(s)}\,x'(s) - \frac{K}{2}F_{sc,y}(x,y) = 0 \end{cases}$$

$$F_{sc,x}(x,y) = 2\frac{1-e^{-r^2/\sigma_r^2}}{r^2}x$$

$$F_{sc,y}(x,y) = 2\frac{1-e^{-r^2/\sigma_r^2}}{r^2}y$$

Many test particles with different initial conditions

(phase plane x/r_b-x′ , y/r_b-y′ , x/r_b- y/r_b)

Halo formation of transverse particle-core model

Gaussian density charged particle motions of matched beam

All points are plotted **in every S lattice period** (Poincare surface of section plots) with different particle initial conditions for propagation **over 300 lattice periods**

Transverse particle motions (real frame)

Coupled equation of motion

$$\begin{cases} x''(s) - 2\sqrt{\kappa_z(s)}\,y'(s) - \frac{K}{2}F_{sc,x}(x,y) = 0 \\ y''(s) + 2\sqrt{\kappa_z(s)}\,x'(s) - \frac{K}{2}F_{sc,y}(x,y) = 0 \end{cases}$$

$$F_{sc,x}(x,y) = 2\frac{1-e^{-r^2/\sigma_r^2}}{r^2}x$$

$$F_{sc,y}(x,y) = 2\frac{1-e^{-r^2/\sigma_r^2}}{r^2}y$$

Many test particles with different initial conditions

(phase plane x/r_b-x′ , y/r_b-y′ , x/r_b- y/r_b)

K=3 , $\sigma_0 = 45.5°$, $\sigma = 12°$ $\frac{\sigma}{\sigma_0} = 0.26$

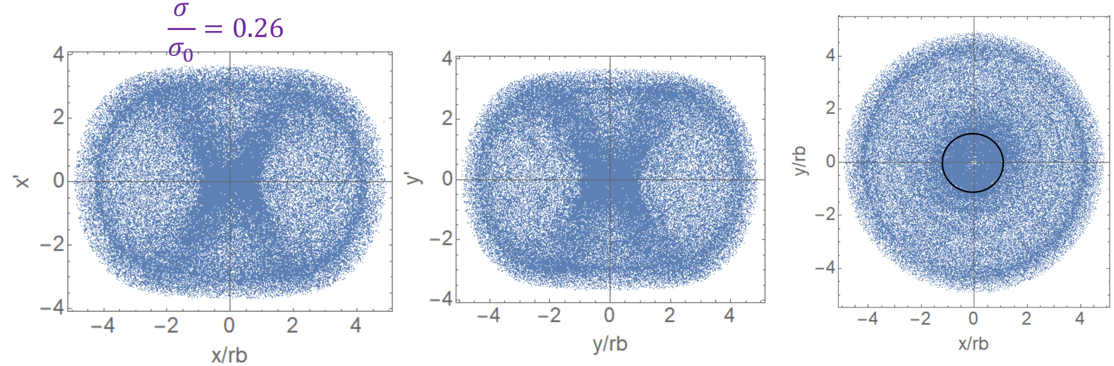

K=2.3 , $\sigma_0 = 115°$, $\sigma = 90°$ $\frac{\sigma}{\sigma_0} = 0.78$

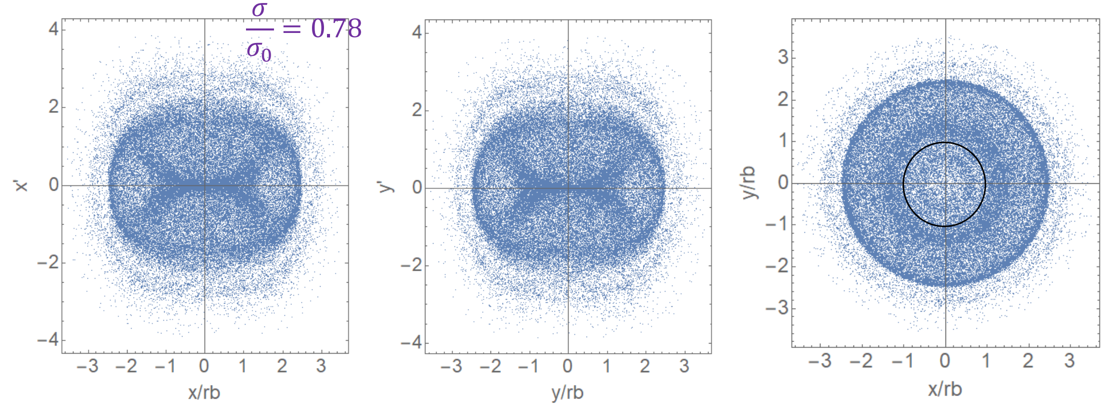

Halo formation of transverse particle-core model

Gaussian density charged particle motions of matched beam

All points are plotted **in every S lattice period** (Poincare surface of section plots) of a single particle for propagation **over 300 lattice periods**

Transverse particle motions

(real frame)

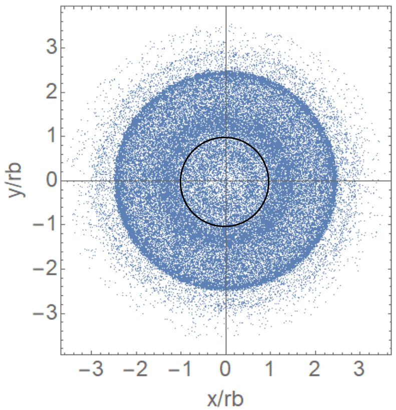

Halo formation of transverse particle-core model

Gaussian density charged particle motions of matched beam

All points are plotted **in every S lattice period** (Poincare surface of section plots) of a single particle for propagation **over 300 lattice periods**

Transverse particle motions

(real frame)

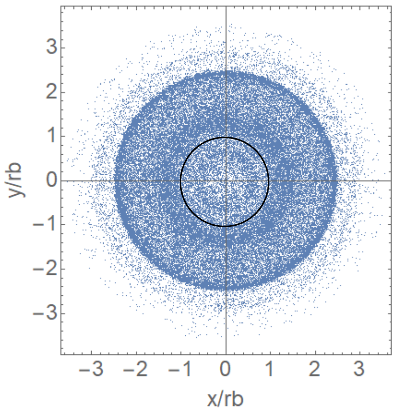

Single test particle motion

(phase plane x/r_b - y/r_b)

K=2.3 , $\sigma_0 = 115°$, $\sigma = 90°$

$$\frac{\sigma}{\sigma_0} = 0.78$$

Halo formation of transverse particle-core model

All points are plotted **in every S lattice period** (Poincare surface of section plots) of a single particle for propagation **over 300 lattice periods**

Gaussian density charged particle motions of matched beam

Transverse particle motions

(real frame)

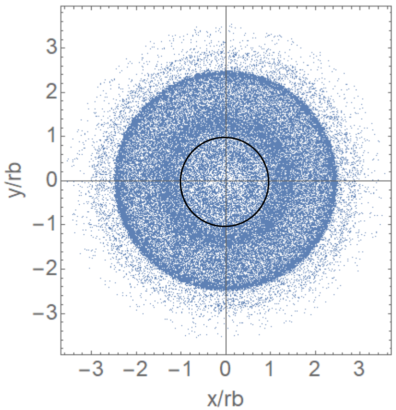

initial condition $\left(\frac{x}{r_b}\right)^2 + \left(\frac{y}{r_b}\right)^2 = (0.1)^2$

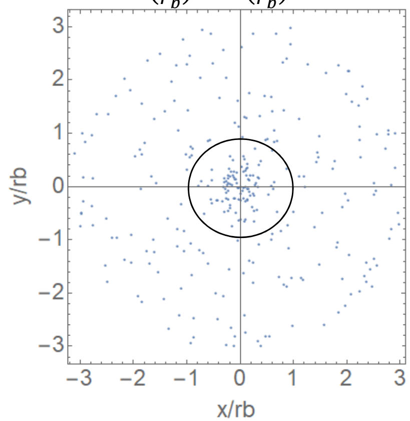

Single test particle motion

(phase plane x/r_b- y/r_b)

K=2.3 , $\sigma_0 = 115°$, $\sigma = 90°$

$\frac{\sigma}{\sigma_0} = 0.78$

Halo formation of transverse particle-core model

All points are plotted **in every S lattice period** (Poincare surface of section plots) of a single particle for propagation **over 300 lattice periods**

Gaussian density charged particle motions of matched beam

Transverse particle motions

(real frame)

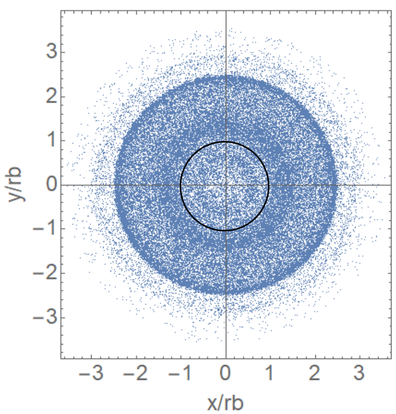

Single test particle motion

(phase plane x/r_b- y/r_b)

$K=2.3$, $\sigma_0 = 115°$, $\sigma = 90°$

$$\frac{\sigma}{\sigma_0} = 0.78$$

initial condition $\left(\frac{x}{r_b}\right)^2 + \left(\frac{y}{r_b}\right)^2 = (0.1)^2$

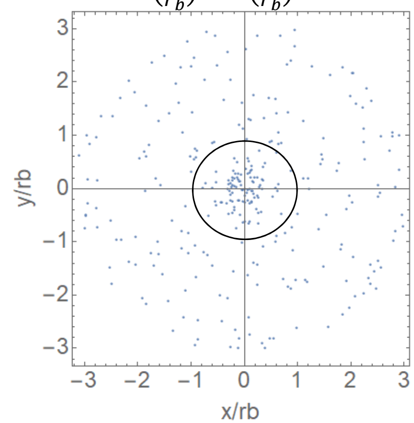

$\left(\frac{x}{r_b}\right)^2 + \left(\frac{y}{r_b}\right)^2 = (0.7)^2$

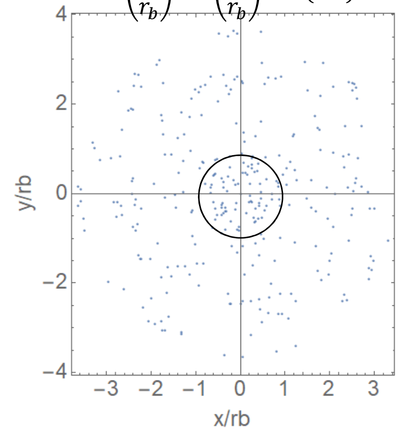

Halo formation of transverse particle-core model

All points are plotted **in every S lattice period** (Poincare surface of section plots) of a single particle for propagation **over 300 lattice periods**

Gaussian density charged particle motions of matched beam

Transverse particle motions

(real frame)

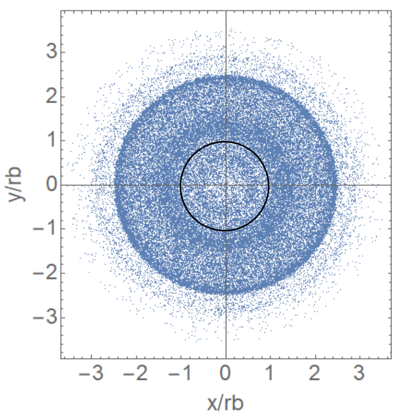

Single test particle motion

(phase plane x/r_b- y/r_b)

K=2.3 , $\sigma_0 = 115°$, $\sigma = 90°$

$$\frac{\sigma}{\sigma_0} = 0.78$$

initial condition $\left(\frac{x}{r_b}\right)^2 + \left(\frac{y}{r_b}\right)^2 = (0.1)^2$

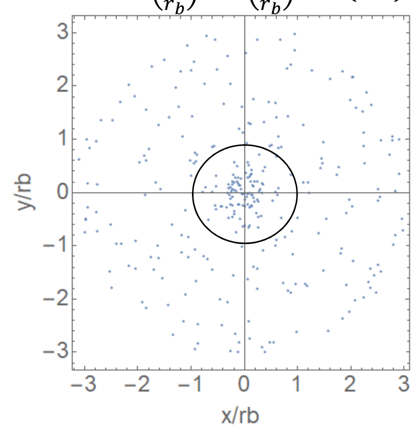

$\left(\frac{x}{r_b}\right)^2 + \left(\frac{y}{r_b}\right)^2 = (0.7)^2$

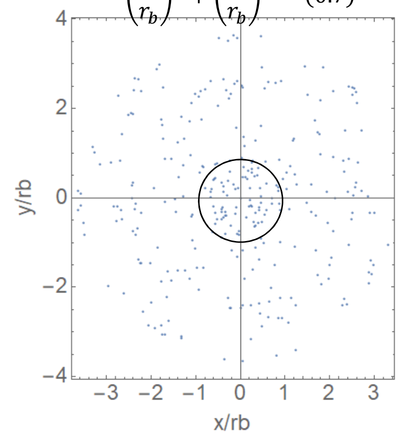

$\left(\frac{x}{r_b}\right)^2 + \left(\frac{y}{r_b}\right)^2 = (0.9)^2$

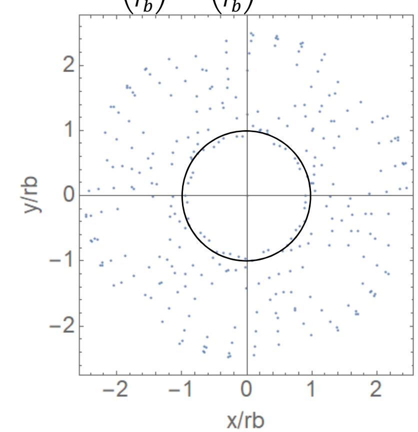

Halo formation of transverse particle-core model

All points are plotted **in every S lattice period** (Poincare surface of section plots) of a single particle for propagation **over 300 lattice periods**

Gaussian density charged particle motions of matched beam

Transverse particle motions

(real frame)

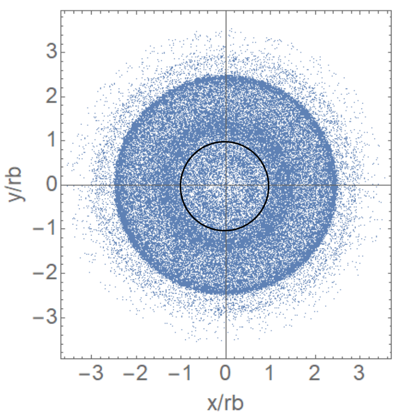

Single test particle motion

(phase plane x/r_b- y/r_b)

K=2.3 , $\sigma_0 = 115°$, $\sigma = 90°$

$\frac{\sigma}{\sigma_0} = 0.78$

initial condition $\left(\frac{x}{r_b}\right)^2 + \left(\frac{y}{r_b}\right)^2 = (0.1)^2$

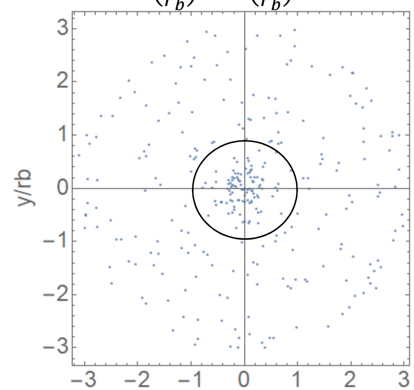

$\left(\frac{x}{r_b}\right)^2 + \left(\frac{y}{r_b}\right)^2 = (0.7)^2$

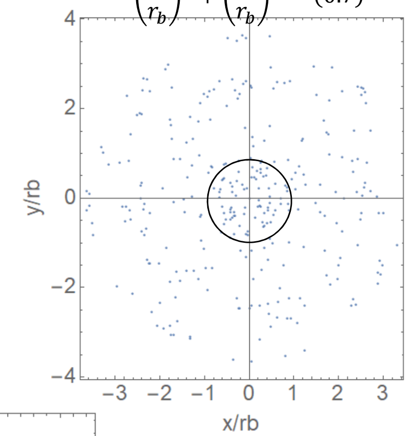

$\left(\frac{x}{r_b}\right)^2 + \left(\frac{y}{r_b}\right)^2 = (0.9)^2$

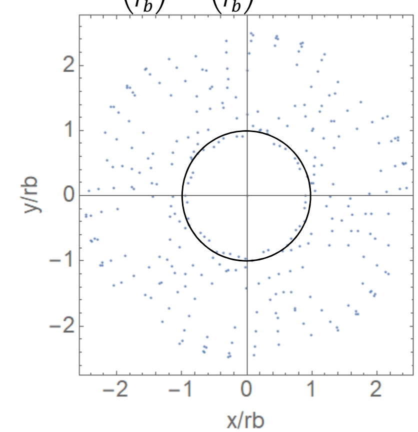

$\left(\frac{x}{r_b}\right)^2 + \left(\frac{y}{r_b}\right)^2 = (1.2)^2$

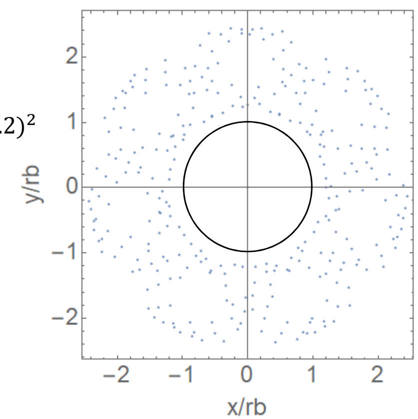

Halo formation of transverse particle-core model

All points are plotted **in every S lattice period** (Poincare surface of section plots) of a single particle for propagation **over 300 lattice periods**

Gaussian density charged particle motions of matched beam

Transverse particle motions

(real frame)

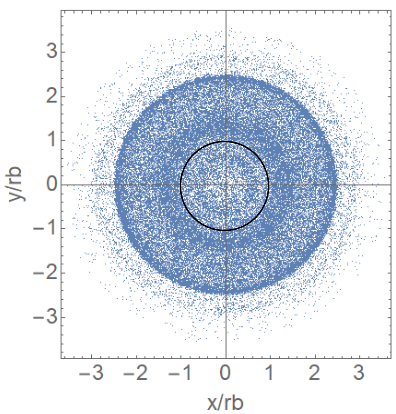

Single test particle motion

(phase plane x/r_b- y/r_b)

K=2.3 , $\sigma_0 = 115°$, $\sigma = 90°$

$\frac{\sigma}{\sigma_0} = 0.78$

initial condition $\left(\frac{x}{r_b}\right)^2 + \left(\frac{y}{r_b}\right)^2 = (0.1)^2$

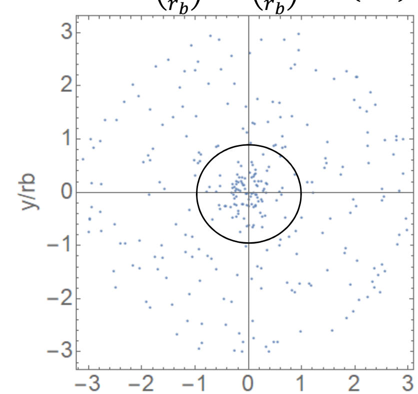

$\left(\frac{x}{r_b}\right)^2 + \left(\frac{y}{r_b}\right)^2 = (0.7)^2$

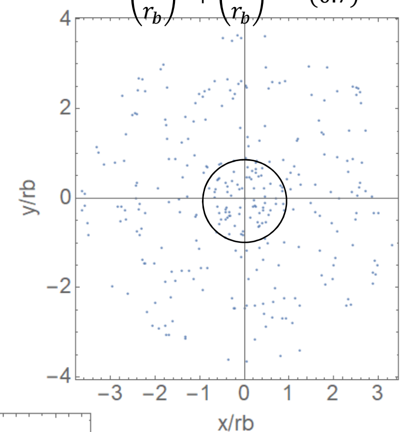

$\left(\frac{x}{r_b}\right)^2 + \left(\frac{y}{r_b}\right)^2 = (0.9)^2$

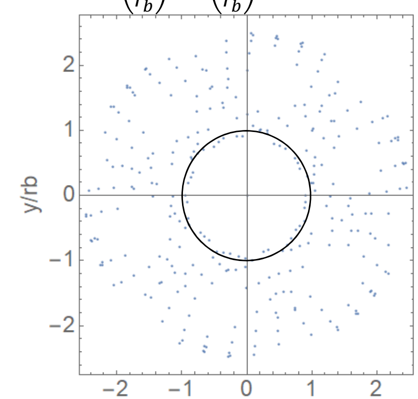

$\left(\frac{x}{r_b}\right)^2 + \left(\frac{y}{r_b}\right)^2 = (1.2)^2$

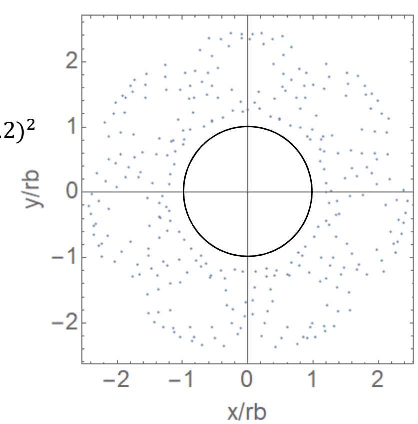

$\left(\frac{x}{r_b}\right)^2 + \left(\frac{y}{r_b}\right)^2 = (2.2)^2$

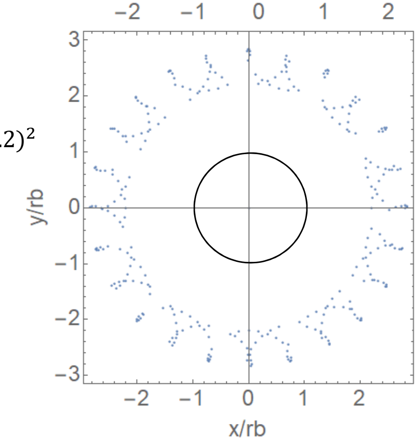

Contents

Summary

Summary

- The periodic solenoidal focusing field is important for several reasons.

Summary

- The periodic solenoidal focusing field is important for several reasons.
- Halo formations

Summary

- The periodic solenoidal focusing field is important for several reasons.
- Halo formations
  - ✓ Uniform charge density

Summary

- The periodic solenoidal focusing field is important for several reasons.

- Halo formations

  ✓ Uniform charge density

<table>
<tr><td rowspan="2">Envelope</td><td>Mis-matched</td><td rowspan="2">Beam core oscillates because of initial mismatch
&
Space charge effect</td><td rowspan="2">Envelope oscillation

Particle frequency</td></tr>
<tr><td>n-th order resonance</td></tr>
</table>

Summary

- The periodic solenoidal focusing field is important for several reasons.
- Halo formations
  - ✓ Uniform charge density

<table>
<tr><td rowspan="2">Envelope</td><td>Mis-matched</td><td rowspan="2">Beam core oscillates because of initial mismatch
&
Space charge effect</td><td rowspan="2">Envelope oscillation
↕ **Resonance**
Particle frequency</td></tr>
<tr><td>n-th order resonance</td></tr>
</table>

Summary

- The periodic solenoidal focusing field is important for several reasons.
- Halo formations

✓ Uniform charge density

Envelope	Mis-matched	Beam core oscillates because of initial mismatch & Space charge effect	Envelope oscillation ↕ **Resonance** Particle frequency
	n-th order resonance		

✓ Non-uniform charge density (**Gaussian**)

Summary

- The periodic solenoidal focusing field is important for several reasons.

- Halo formations

  ✓ Uniform charge density

Envelope	Mis-matched	Beam core oscillates because of initial mismatch & Space charge effect	Envelope oscillation ↕ **Resonance** ↕ Particle frequency
	n-th order resonance		

  ✓ Non-uniform charge density (**Gaussian**)

Envelope	Matched	Gaussian density profile	**Non-linear space charge force**

Summary

- The periodic solenoidal focusing field is important for several reasons.

- Halo formations

✓ Uniform charge density

<table>
<tr><td rowspan="2">Envelope</td><td>Mis-matched</td><td rowspan="2">Beam core oscillates because of initial mismatch
&
Space charge effect</td><td rowspan="2">Envelope oscillation
↕ Resonance
Particle frequency</td></tr>
<tr><td>n-th order resonance</td></tr>
</table>

✓ Non-uniform charge density (**Gaussian**)

Envelope	Matched	Gaussian density profile	**Non-linear space charge force**

- Symmetric gaussian -> radial motion
- Non symmetric gaussian -> coupled motions of x, y -> many test particles / single particle motions

Future plan

Reference

- Chen, C., & Davidson, R. C. (1994). "Nonlinear resonances and chaotic behavior in a periodically focused intense charged-particle beam." *Physical review letters*, *72*(14), 2195.
- Ikegami, M. (1999). "Particle-core analysis of mismatched beams in a periodic focusing channel." *Physical Review E*, *59*(2), 2330.
- Wangler, T. P., Crandall, K. R., Ryne, R., & Wang, T. S. (1998). "Particle-core model for transverse dynamics of beam halo." *Physical review special topics-accelerators and beams*, *1*(8), 084201.
- Groening, L., Hofmann, I. (2011). "Experimental observation of space charge driven resonances in a linac."
- Qian, Q., Davidson, R. C., & Chen, C. (1995). "Chaotic particle motion and halo formation induced by charge nonuniformities in an intense ion beam propagating through a periodic quadrupole focusing field." *Physics of Plasmas*, *2*(7), 2674-2686.

Future plan

- Transverse particle beam dynamics
  - particle-core model compare with PIC simulation of self-consistence
- Longitudinal beam dynamics
- Apply to the beam halo and beam loss measurement design input

Reference

- Chen, C., & Davidson, R. C. (1994). "Nonlinear resonances and chaotic behavior in a periodically focused intense charged-particle beam." *Physical review letters*, *72*(14), 2195.
- Ikegami, M. (1999). "Particle-core analysis of mismatched beams in a periodic focusing channel." *Physical Review E*, *59*(2), 2330.
- Wangler, T. P., Crandall, K. R., Ryne, R., & Wang, T. S. (1998). "Particle-core model for transverse dynamics of beam halo." *Physical review special topics-accelerators and beams*, *1*(8), 084201.
- Groening, L., Hofmann, I. (2011). "Experimental observation of space charge driven resonances in a linac."
- Qian, Q., Davidson, R. C., & Chen, C. (1995). "Chaotic particle motion and halo formation induced by charge nonuniformities in an intense ion beam propagating through a periodic quadrupole focusing field." *Physics of Plasmas*, *2*(7), 2674-2686.

Thank you for your attention !

61th ICFA Advanced Beam Dynamics Workshop
on High-intensity and High-brightness Hadron beams (**HB 2018**)
In Daejeon

Yoolim Cheon and Moses Chung,
Intense Beam and Accelerator Laboratory (IBAL),
Ulsan National Institute of Science and Technology (UNIST)